cosmetics

MDPI

Article

Concurrent Changes in Facial Skin Parameters, Sleep, and the Salivary Melatonin Day–Night Difference During Topical Use of a Clock-Oriented Six-Botanical Formulation: An Exploratory 4-Week, Single-Arm Pilot Study

Miji Yeom [1], Youngsu Jang [1], Kyungeun Jeon [1], Yoon Ji Jeong [2], Soeun Cho [2], Heetae Kim [2], Sunhong Moon [1], De-Hun Ryu [1], Eunae Cho [1], Deokhoon Park [1] and Eunsun Jung [1,*]

[1] BioSpectrum Inc., Life Science Institute, A-1805, U-TOWER, 767, Sinsu-ro, Suji-gu, Yongin-si 16827, Gyeonggi-do, Republic of Korea; biout@biospectrum.com (M.Y.); biogc@biospectrum.com (Y.J.); bioyd@biospectrum.com (K.J.); bioyo@biospectrum.com (S.M.); biosc@biospectrum.com (D.-H.R.); biozr@biospectrum.com (E.C.); pdh@biospectrum.com (D.P.)

[2] Dermacle Skin Research Center for Clinical Test of Cosmetics, A-1606, U-TOWER, 767, Sinsu-ro, Suji-gu, Yongin-si 16827, Gyeonggi-do, Republic of Korea; dm13@dermacle.com (Y.J.J.); dm11@dermacle.com (S.C.); htkim@dermacle.com (H.K.)

* Correspondence: bioso@biospectrum.com; Tel.: +82-70-5117-0029

Abstract

Insufficient sleep can disrupt circadian organization and adversely affect skin condition. Perturbation of the cutaneous clock, which governs skin homeostasis, may contribute to this deterioration. In our study, a six-botanical mixture extract increased *PER2* promoter-driven luciferase output in HaCaT keratinocytes, and reduced *IL6* and *CXCL10* expression, two PER2-associated inflammatory mediators. Separately, a 4-week single-arm pilot study evaluated a cream containing 2.00% (*w*/*w*) of a liquid preparation of this extract, applied nightly by 22 women aged 40–70 years with poor sleep quality. Skin indicators, sleep, mood, and salivary melatonin and cortisol were assessed as changes from baseline at week 4. The 13 skin indicators changed from baseline across the anti-aging, barrier, complexion, and dark-circle categories (Cohen's *d* 0.47–4.81). Sleep duration increased, whereas PSQI-K and PHQ-9 scores decreased; the melatonin day–night difference increased ($d = 0.75$); cortisol measures did not change significantly. No adverse skin reactions were reported. These exploratory findings do not establish product-attributable efficacy or a causal PER2-mediated mechanism; placebo, vehicle, expectancy, seasonal, behavioral, and regression-to-the-mean effects cannot be excluded. A randomized, vehicle-controlled study is required, with prespecified primary outcomes, denser circadian sampling, and clock activity measured directly in treated skin.

Keywords: PER2; circadian rhythm; skin aging; skin barrier; plant extract; sleep quality; melatonin; dark circles; skin–brain axis

Academic Editor: Enzo Berardesca

Received: 7 September 2026
Revised: 30 October 2026
Accepted: 31 October 2026
Published: 4 November 2026

Copyright: © 2026 by the authors. Licensee MDPI, Basel, Switzerland. This article is an open access article distributed under the terms and conditions of the Creative Commons Attribution (CC BY) license.

1. Introduction

Sleep is among the lifestyle factors that influence skin condition [1]. Poor sleep quality is associated with disturbances in systemic circadian organization and with deterioration in skin condition. In objective assessments, poorer sleep quality has been linked

consistently with reduced barrier function, elevated transepidermal water loss (TEWL), accelerated signs of visible aging, dyspigmentation, and periorbital changes such as dark circles [2–6]. In an experimental study, restricting sleep to 4 h per night for six consecutive nights reduced skin hydration, gloss, transparency, and elasticity and worsened desquamation, texture, and wrinkles in Korean women in their forties [7]. In particular, sleep disturbance has been reported in association with higher circulating concentrations of inflammatory markers, including C-reactive protein and interleukin-6 (IL-6) [8]. Experimental sleep loss also alters clock gene expression and circadian transcription in peripheral human tissues such as blood, indicating that sleep–wake behavior contributes to the temporal organization of peripheral oscillators [9–11]. In mice, prolonged sleep deprivation altered core clock gene expression in skin tissue and was accompanied by impaired epidermal tight junctions and reduced dermal collagen [12]; sleep restriction likewise weakened the oscillation of the skin clock, alongside barrier damage and oxidative stress in the skin [13]. Direct evidence for such changes in the skin of individuals with poor sleep quality remains limited. The skin, however, is itself a peripheral tissue with a cell-autonomous oscillator, and cutaneous clock regulation therefore represents a biologically relevant framework for studying skin deterioration in this population.

A circadian clock is an endogenous timekeeping mechanism that aligns biological processes with the external day, so that each occurs at the time best suited to it [9]. The peripheral oscillator in the skin has been characterized in some detail: beyond responding to the central pacemaker in the suprachiasmatic nucleus (SCN), the skin is a clock-controlled tissue in which the core clock genes *PER1/2*, *CRY1/2*, *BMAL1*, and *CLOCK* are expressed in keratinocytes, fibroblasts, and melanocytes [9,14,15], and in which roughly a tenth of the skin transcriptome oscillates over the day [16]. Studies in human skin-derived models indicate that clock signaling contributes to barrier function and differentiation, extracellular matrix turnover, epidermal renewal and antioxidant defense [17,18], pigmentation, and inflammatory signaling [9,14,17–19]. In cultured human keratinocytes, PER-associated clock signaling contributes to suppressing matrix metalloproteinase-1 (MMP-1) expression [20], and barrier- and differentiation-related genes are transcriptionally coupled to clock gene activity [21,22]. Cell-autonomous clock activity has been implicated in restraining melanogenesis in human skin and melanocyte models [23], and in suppressing inflammatory mediator expression in human keratinocytes [17], consistent with clock–NF-κB crosstalk [19]. Loss-of-function studies in mice indicate that this regulation is functionally required: keratinocyte-specific deletion of *Bmal1* abolishes the time-of-day synchronization of epidermal cell division and leaves proliferation constitutively elevated [24], and *Bmal1*-deficient animals heal epidermal wounds more slowly, with accumulation of reactive oxygen species [25]. Consistent with these cellular and molecular findings, the physiology of human skin is also temporally organized, with TEWL, surface pH, and temperature following reproducible 24 h profiles in vivo [26]. Taken together, these findings support the view that the skin clock temporally coordinates repair, regeneration, and environmental defense, and they provide a biological basis for interpreting the signs of aging, barrier function, complexion, and periorbital appearance assessed in cosmetic studies.

The skin is not only a passive barrier but a tissue in which sensory, immune, and neuroendocrine signaling intersect [27]. Cytokines released by keratinocytes and immune cells, and neuropeptides released from activated sensory nerve endings, can engage local neural and humoral routes that connect the tissue to central and systemic regulatory networks [28–31]. Signaling also runs in the opposite direction, in that cortisol, melatonin, and the sleep–wake state that shapes their daily profiles act on cutaneous barrier and immune function [29,30,32]. This bidirectional biology, increasingly framed as the skin–brain axis [33], provides a rationale for assessing sleep, mood, and salivary melatonin and

cortisol alongside skin endpoints. In atopic dermatitis, improvements in skin disease severity and in sleep quality have been observed to occur together [34]. A topical product containing a fraction obtained from *Melaleuca alternifolia* (tea tree) essential oil has been reported to improve both sleep quality and signs of skin aging [35].

The formulation evaluated in the present study is built on a blend of extracts from six botanicals: hop, chamomile, ginseng, rosemary, loquat leaf, and citrus peel. Their principal constituents—the hop bitter acids humulone and lupulone together with xanthohumol, chamomile α-bisabolol, chamazulene, and apigenin, ginsenosides, rosemary rosmarinic and carnosic acids, loquat pentacyclic triterpenes such as ursolic acid, and citrus hesperetin, narirutin, and nobiletin—have documented activity in skin, including anti-inflammatory and antioxidant effects [36–41].

Drawing on these clinical, mechanistic, and botanical lines of evidence, the present study evaluated this blend, characterized in vitro by increased *PER2* promoter-driven luciferase output, as a topical formulation in a population with poor sleep quality. We conducted a 4-week, single-arm, open-label pilot trial in 22 adult women aged 40 to 70 years with poor sleep quality, defined as a score of 7 or higher on the Korean version of the Pittsburgh Sleep Quality Index (PSQI-K). The study addressed two objectives. The first was to characterize the changes in 13 skin indicators spanning four functional categories—anti-aging, barrier, complexion, and dark circles—during use of the topical formulation in this cohort with poor sleep quality. The second was to explore whether changes in skin outcomes were accompanied by changes in sleep, mood, and salivary biomarkers over the same period.

2. Materials and Methods

2.1. Preparation of the Test Materials

The test material was prepared in three stages: extraction of the six individual botanicals, combination of the dried extracts in fixed proportions by weight to give a six-botanical mixture extract, and dissolution of that mixture extract to give the liquid preparation RhythmiQ Blend.

For the individual extracts, six botanicals were used, including non-edible plant parts: hop flower (*Humulus lupulus*; K-Hops, Hongcheon, Gangwon, Republic of Korea), chamomile flower (*Matricaria chamomilla*; Herb Kingdom, Namwon, Jeonbuk, Republic of Korea), ginseng root (*Panax ginseng*; Korea Ginseng, Geumsan, Chungcheongnam-do, Republic of Korea), rosemary leaf (*Rosmarinus officinalis*; Jirion, Namwon, Jeonbuk, Republic of Korea), loquat leaf (*Eriobotrya japonica*; a local grower, Jeju, Republic of Korea), and citrus peel (*Citrus unshiu*; Saengdeure, Jocheon, Jeju, Republic of Korea). Each botanical was washed, shade-dried at 20 to 35 °C, and pulverized to a particle size of 1 mm or less. To each pulverized material, 70% ethanol (Merck, Darmstadt, Germany) was added at ten times the weight of the material (a 10:1 solvent-to-material ratio), and extraction was carried out at 80 °C for 3 h. Each extract was then concentrated under reduced pressure and dried to a powder. Yields, expressed as dried extract per raw material (% *w*/*w*), were 37.5 for hop, 14.6 for chamomile, 7.4 for ginseng, 2.6 for rosemary, 13.3 for loquat, and 4.4 for citrus.

The six dried extracts were then blended at a weight ratio of 1:5:8:2:2:2 for hop, chamomile, ginseng, rosemary, loquat, and citrus, respectively, to give the six-botanical mixture extract. This mixture extract was the material used in the in vitro experiments.

For the clinical study, the mixture extract was dissolved in a solvent system of butylene glycol, water, and polyglyceryl-10 oleate to give the liquid preparation, which contained the mixture extract at 0.5% (*w*/*w*) and was then incorporated into the test cream at 2.00% (*w*/*w*).

A single production lot of the liquid preparation (Lot 102251004) was used for all characterization and for the cream applied in the clinical study. Chlorogenic acid and rosmarinic acid were quantified in the liquid preparation as marker compounds by high-performance liquid chromatography with photodiode-array detection at 325 nm on a HydroRP column (250 × 4.6 mm, 4 μm; Phenomenex, Torrance, CA, USA) held at room temperature, with a gradient of acetonitrile in aqueous 0.1% trifluoroacetic acid rising from 10% to 100% over 55 min at a flow rate of 1.0 mL/min and an injection volume of 10 μL. The liquid preparation was analyzed undiluted, and the two compounds were quantified against five-point external calibration curves prepared from authentic standards (Sigma-Aldrich, St. Louis, MO, USA), with every calibration level and the sample injected in triplicate; calibration was linear over 5 to 103 μg/mL (R [2] = 1.000), and the limits of quantification were 2.2 μg/g for chlorogenic acid and 2.3 μg/g for rosmarinic acid. The stability of the liquid preparation was tested on the same lot. In a short-term test it met the acceptance criteria for appearance, color, odor and pH after 3 days at 70 °C and after 6 h of exposure to ultraviolet A at 40 W/m [2] (320 to 400 nm), each against a control held at room temperature in the dark. In a long-term test, it met the acceptance criteria for color, odor and pH at 8 weeks under storage at 4 °C, 25 °C, and 45 °C and under a temperature-cycling condition of 24 h cycles through 25, 37, 45, 25, and 4 °C with 4.5 h at each step. The test cream itself was not subjected to stability testing.

2.2. In Vitro Experiments

2.2.1. Cell Culture and Treatment

Two cell lines were used: HaCaT (CLS Cell Line Service GmbH, Eppelheim, Germany), a spontaneously immortalized human keratinocyte line, and a HaCaT-derived reporter line stably expressing a *PER2* promoter–driven luciferase construct (PER2pro-LUC), which had been established previously [20]. Both lines were maintained in Dulbecco's Modified Eagle's Medium (DMEM; Welgene, Gyeongsan, Republic of Korea) supplemented with 10% fetal bovine serum (FBS; 16000044; Gibco, Grand Island, NY, USA) and 1% penicillin/streptomycin (15140122; Invitrogen, Carlsbad, CA, USA), and were held at 37 °C in a humidified atmosphere of 5% CO_2. For treatment, cells were seeded in growth medium, grown to the confluence specified for each assay, and then exposed to the six-botanical mixture extract in DMEM containing 1% FBS for 24 h or 48 h. The mixture extract was dissolved in dimethyl sulfoxide (DMSO; Duchefa Biochemie, Haarlem, Netherlands) and applied at final concentrations of 10, 25, and 50 μg/mL, with DMSO held at 0.1% (*v*/*v*) in all conditions as the vehicle control, following procedures described previously [22].

2.2.2. *PER2* Promoter–Reporter Assay

To monitor *PER2* promoter-driven luciferase output in live cells, PER2pro-LUC reporter cells were seeded into white 96-well plates (655083; Greiner Bio-One, Monroe, NC, USA). Once the cells reached confluence, the clock was synchronized by a 1 h pulse of 1 μM dexamethasone (D1756; Sigma-Aldrich, St. Louis, MO, USA) in DMEM, after which the cells were treated with the mixture extract at the indicated concentrations for 24 h as described above. The medium was then exchanged for a recording medium composed of DMEM with 1% FBS, 1% penicillin/streptomycin, 10 mM HEPES (pH 7.4; 15630080; Gibco, Grand Island, NY, USA), 0.2 mg/mL hygromycin (H0192.0001; Duchefa Biochemie, Haarlem, Netherlands), and 1 mM luciferin (LUCK-1G; Goldbio, St. Louis, MO, USA), without the mixture extract. Bioluminescence was recorded at hourly intervals for 72 h on an Infinite M200 microplate reader (Tecan, Männedorf, Switzerland). For rhythm analysis, each trace was detrended by subtracting a 24 h moving average, smoothed with a 3 h moving average, and analyzed in BioDare2 (https://biodare2.ed.ac.uk/, accessed on 31 August 2026) over 16 to 72 h by the fast Fourier transform–nonlinear least squares (FFT NLLS)

method, which returned the amplitude of each trace. Peak bioluminescence was determined separately for each of the three circadian cycles resolved within the recording, taken as the maximum of the recorded signal within 0 to 18 h, 18 to 40 h, and 42 to 68 h.

2.2.3. *PER2* Knockdown

For gene silencing, HaCaT cells were seeded in 12-well white plates and, at approximately 60% confluence, transfected with 10 nM of either a *PER2*-targeting small interfering RNA (siRNA) (sc-36209) or a non-targeting control siRNA (sc-37007; both from Santa Cruz Biotechnology, Dallas, TX, USA) using Lipofectamine RNAiMAX (13778-075; Invitrogen, USA) in Opti-MEM (31985062; Gibco, Grand Island, NY, USA), according to the manufacturer's instructions; cells were harvested 48 h after transfection for transcript analysis.

2.2.4. RNA Extraction and Quantitative Real-Time PCR

Total RNA was isolated with the TaKaRa MiniBEST Universal RNA Extraction Kit (9767A; Takara Bio, Kusatsu, Shiga, Japan), and 1 μg of total RNA was reverse-transcribed into complementary DNA using amfiRivert cDNA Synthesis Platinum Master Mix (R5600; GenDEPOT, Barker, TX, USA). Quantitative real-time reverse transcription polymerase chain reaction (RT-PCR) was performed on a CronoSTAR 96 Real-Time PCR system (Takara Bio, Japan) according to the manufacturer's protocol, as described previously [22]. Transcript levels of interleukin 6 (*IL6*), C-X-C motif chemokine ligand 10 (*CXCL10*), and *PER2* were quantified by the $2^{-\Delta\Delta Ct}$ method, normalized to *PUM1* as the reference gene and expressed relative to the corresponding vehicle or non-targeting control of the same experiment, so that the control equals 1; the primer sequences are listed in Table 1.

Table 1. Primer sequences used for quantitative real-time RT-PCR.

Gene	Accession No.	Direction	Sequence (5′ → 3′)
IL6	NM_000600	Forward	ACAACCTGAACCTTCCAAAG
		Reverse	CCTCAAACTCCAAAAGACCAG
CXCL10	NM_001565	Forward	GCAGTTAGCAAGGAAAGGTC
		Reverse	TGTAGGGAAGTGATGGGAG
PER2	NM_022817.2	Forward	GACTGCAAACCTGGCACTTC
		Reverse	GTGTCTGAGGGTTCATCACG
PUM1	NM_001020658.2	Forward	CGGTCGTCCTGAGGATAAAA
		Reverse	CGTACGTGAGGCGTGAGTAA

Abbreviations: RT-PCR, reverse transcription polymerase chain reaction. *PUM1* was used as the reference (housekeeping) gene for normalization.

2.2.5. Cell Viability Assay

To establish that differences in reporter signal were not attributable to differences in the number or metabolic state of the cells, viability was assessed by reduction of 3-(4,5-dimethylthiazol-2-yl)-2,5-diphenyltetrazolium bromide (MTT) as described previously [22]. Cells treated in parallel under the conditions used for the reporter assay were incubated with MTT reagent (Invitrogen) at the time of the second bioluminescence peak, 27 h after the medium exchange; the formazan was then dissolved in DMSO and the absorbance measured at 570 nm on an Epoch microplate reader (BioTek, Winooski, VT, USA). Values are expressed relative to the DMSO control.

2.2.6. In Vitro Statistical Analysis

Data are presented as the mean ± standard deviation (SD) of three independent experiments (n = 3 per group), which constitute the biological replicates; within each

experiment, every condition was assayed in technical triplicate wells, and the three wells were averaged to give a single measurement per condition before analysis. All treatment conditions were evaluated concurrently within each independent experiment. Differences among matched treatment conditions were analyzed using one-way repeated-measures analysis of variance (ANOVA), followed by Dunnett's multiple-comparisons test comparing each concentration of the mixture extract with the DMSO control; the Dunnett-adjusted comparisons were calculated using the residual mean square from the randomized-block ANOVA, with the independent experimental run treated as the blocking factor. Concentration dependence was tested with a linear contrast across the four concentrations, evaluated against the same residual mean square. The same model was applied to the peak bioluminescence of each cycle, with the three cycles analyzed as separate families, and to the viability data. For the endogenous *PER2* mRNA measurements, which comprised three matched conditions (vehicle and the mixture extract at 10 and 50 μg/mL) at each of two exposure times, the same model was applied separately at each exposure time, with the linear contrast taken across the three concentrations and each exposure time analyzed as a separate family. In the knockdown experiment, the *PER2*-targeting and non-targeting control siRNA conditions were likewise matched within each independent experiment and were compared by a two-tailed paired t-test.

2.3. Clinical Evaluation

2.3.1. Study Design and Ethics

This study was designed as a single-arm, open-label, single-center pilot clinical trial. Participants applied the test cream for 4 weeks; skin indicators were assessed at baseline, week 2, and week 4, whereas the wellness indicators and salivary biomarkers were assessed at baseline and week 4. Each participant served as her own reference, with outcomes evaluated as within-subject changes from baseline.

The study protocol was approved by the Institutional Review Board of Dermacle Co., Ltd. (Yongin, Republic of Korea; Approval No. DM-IRB-2025-1014-04) and was conducted in accordance with the ethical principles of the Declaration of Helsinki. Written informed consent was obtained from every participant before enrollment. The trial was registered with the Clinical Research Information Service (CRIS) of the Republic of Korea (registration No. KCT0011193) on 21 November 2025. Registration was retrospective with respect to the enrollment of the first participant (21 October 2025) because of an administrative oversight in the timing of registration. It was nevertheless completed before the end of data collection (28 November 2025) and before the start of data analysis. The reporting of this non-randomized study follows the TREND statement, and the completed checklist is provided as Supplementary File S1.

2.3.2. Participants

Women aged 40 to 70 years with poor sleep quality were enrolled and screened at the testing institution (Dermacle Co., Ltd., Yongin, Republic of Korea). Sleep quality was screened with the Korean version of the Pittsburgh Sleep Quality Index (PSQI-K), a validated instrument in which a higher global score indicates poorer sleep [42,43]. Reported optimal PSQI-K cut-off scores in Korean validation studies range from 6 to 8.5, depending on the study population and the external reference used [43,44]. Eligibility therefore required a PSQI-K score of 7 or higher, a conservative screening criterion within that range and the criterion used in a previous Korean study of women with sleep complaints that assessed both sleep and skin outcomes [45]. Eligibility also required self-reported insomnia attributed to aging or to climacteric symptoms. Enrolled women also presented with periorbital wrinkles and with dark circles of vascular or pigmentary origin. Exclusion criteria included pregnancy or lactation; skin abnormalities or infectious skin disease at the

test sites; under-eye sagging that could be mistaken for dark circles; allergy, hypersensitivity, or a tendency to irritation from cosmetics, medicines, or light exposure; recent steroid treatment, phototherapy, or dermatological procedures; a psychiatric, intellectual, nutritional, or substance-use disorder; recent participation in the same type of study; and any other condition judged unsuitable by the principal investigator. Participants were recruited through an online advertisement, and recruitment ran from 24 September to 23 October 2025. Of the 75 women who applied and were assessed for eligibility by telephone, 25 attended an on-site screening visit, at which 2 did not meet the PSQI-K criterion. The sample size followed the Korea Ministry of Food and Drug Safety guideline on test methods for the substantiation of cosmetic labeling and advertising, which recommends a minimum of 20 participants, and 23 women were enrolled to allow for potential dropout. One enrolled participant underwent a dermatological procedure after enrollment but before the baseline visit, which met the exclusion criterion on dermatological procedures within 3 months; she was therefore withdrawn before that visit and contributed no data to any analysis. No participant withdrew after starting to use the test cream; all 22 participants who began application completed the study, and all analyses were performed on these 22 participants (mean age, 53.0 years; range, 40–69 years). The flow of participants through the study is shown in Figure 1. None of the skin, questionnaire, or salivary measurements were missing for any of the 22 participants at any scheduled time point; the only incomplete data were two nights of wearable sleep recording, as described in Section 2.3.4. Menopausal status and skin phototype were not recorded.

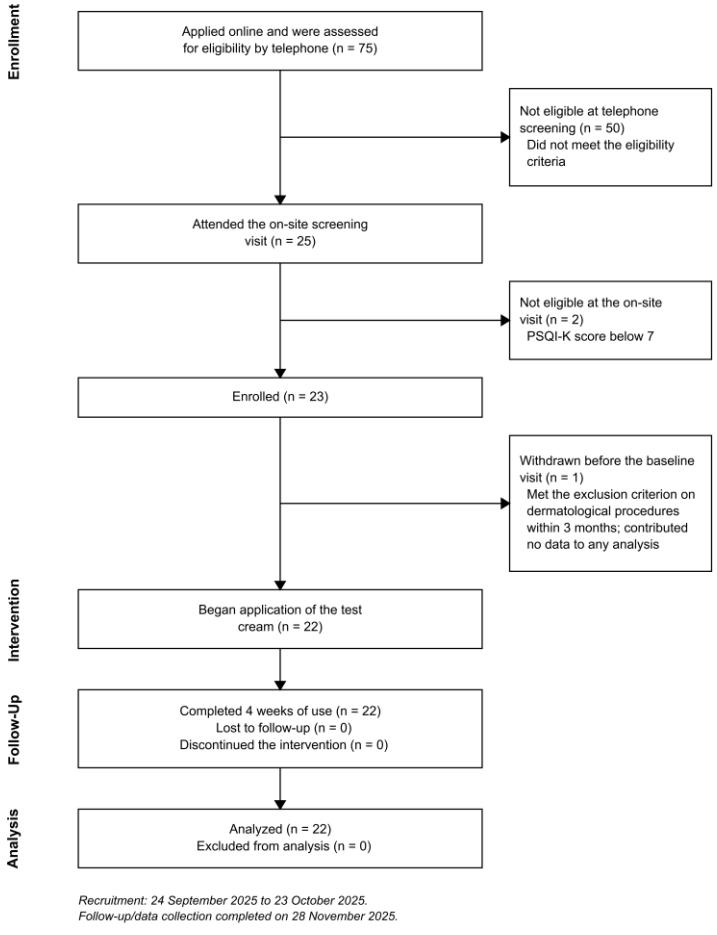


Figure 1. Flow of participants through the study. The diagram traces participants from the telephone eligibility assessment to the final analysis across the enrollment, intervention, follow-up, and analysis stages. The central column gives the number of women at each step, and the boxes on the right

give the number who left the study at that step together with the reason. The recruitment period and the completion date of follow-up are noted below the diagram. PSQI-K, Korean version of the Pittsburgh Sleep Quality Index.

2.3.3. Test Product and Application

For the clinical study, a test cream containing 2.00% (*w*/*w*) of the liquid preparation of the six-botanical mixture extract was used. This corresponds to the mixture extract at 100 μg/g (0.01%, *w*/*w*) of the cream, comprising 5, 25, 40, 10, 10, and 10 μg/g of the hop, chamomile, ginseng, rosemary, loquat, and citrus extracts, respectively. The full qualitative and quantitative composition of the cream, including the International Nomenclature of Cosmetic Ingredients (INCI) designation and functional role of each component, is given in Table 2.

Table 2. Qualitative and quantitative composition of the test cream containing 2.00% (*w*/*w*) RhythmiQ Blend.

Phase	Trade Name	INCI Name	Function	Content (% *w*/*w*)
A	Water	Water	Solvent	To 100
A	RhythmiQ Blend [a]	Butylene Glycol, Water, Polyglyceryl-10 Oleate, Panax Ginseng Root Extract, Chamomilla Recutita (Matricaria) Flower Extract, Rosmarinus Officinalis (Rosemary) Leaf Extract, Eriobotrya Japonica Leaf Extract, Citrus Unshiu Peel Extract, Humulus Lupulus (Hops) Extract	Test material	2.00
A-1	Glycerine (RSPO MB)	Glycerin	Humectant	5.00
A-1	Vanzan NF-C	Xanthan Gum	Viscosity controlling agent	0.30
B	Cellike Forte [b]	Caprylic/Capric Triglyceride, Hydrogenated Lecithin, Cetearyl Alcohol, Butyrospermum Parkii (Shea) Butter, Hydrogenated Phosphatidylcholine, Phytosteryl Macadamiate, Cetearyl Olivate, Sorbitan Olivate, Phytosterols, Squalane, Ceramide NP	Natural emulsifier	8.00
B	Lanette O (CSPO)	Cetearyl Alcohol	Consistency factor	2.00
B	Palmsurf MCT 60/40	Caprylic/Capric Triglyceride	Skin conditioning	5.00
B	Sepinov WEO	Hydroxyethyl Acrylate/Sodium Acryloyldimethyl Taurate Copolymer	Thickener	1.00
B-1	Gundenics [b]	Propanediol, Glyceryl Undecylenate, Caprylyl Glycol, Levulinic Acid	Natural preservative	1.20
C	10% Citric acid	Water, Citric Acid	pH adjuster	q.s. [c]

Abbreviations: INCI, International Nomenclature of Cosmetic Ingredients; *w*/*w*, weight/weight; q.s., quantity sufficient. [a] RhythmiQ Blend is the liquid preparation of the six-botanical mixture extract described in the Methods (Preparation of the Test Materials); the listed INCI components comprise the solvent system and the six plant extracts. [b] Product of BioSpectrum Inc. (Yongin-si, Gyeonggi-do, Republic of Korea). [c] q.s., quantity sufficient to adjust the final pH; the final pH of the cream was 5.58.

Participants applied the test cream to the entire face once daily, in the evening after cleansing and before bedtime, for 4 weeks, and the number of applications was checked with a usage diary. The amount of cream applied was not measured. During the study period, participants were asked to refrain from using any other cosmetic or medicinal product that could affect the study outcomes and from taking other drugs that could affect the skin.

2.3.4. Outcome Measures

The outcome measures comprised three domains: 13 skin indicators, 3 wellness indicators, and 6 salivary biomarker comparisons, the last consisting of the daytime and nighttime concentrations of two hormones together with the day–night difference derived from each. The registered protocol did not specify a hierarchy among these outcomes, and no outcome was designated as primary. They are therefore reported without ranking.

Skin indicators. Skin outcomes were evaluated by instrumental measurement at baseline, week 2, and week 4. All measurements were made in a room shielded from direct sunlight and maintained at 22 ± 2 °C and 50 ± 10% relative humidity, and each participant washed her face and then rested for at least 30 min to acclimatize to these conditions before measurement. Visits were scheduled so that each participant was assessed at approximately the same time of day at every visit. The 13 skin indicators were organized into four functional categories, with the measurement site and instrument mode of each indicator as described below. Measurement sites were distributed between the left and the right side of the face to avoid concentrating the measurements on a single area, and each indicator was measured on the same side in every participant and at every visit.

The anti-aging category comprised six indicators. Eye wrinkles were assessed at the left periorbital region using the Antera 3D CS (Miravex Limited, Dublin, Ireland) in Wrinkles mode (yielding quantitative indices such as the indentation index), and skin volume was assessed at the left cheek using the same device in Volumes mode (the volume parameter derived from three-dimensional surface mapping). Skin elasticity and elastic recovery were both measured at the right cheek with the Cutometer dual MPA580 (Courage + Khazaka electronic GmbH, Cologne, Germany) and expressed as the R2 and R7 parameters, respectively: R2 = Ua/Uf, the ratio of the total deformation recovery at the end of the suction-off period (Ua) to the maximal deformation (Uf), and R7 = Ur/Uf, the ratio of the elastic recovery immediately after release of the suction (Ur) to the maximal deformation, both expressed as percentages [46]. The skin lifting angle was obtained by facial imaging with the F-ray system (BeYoung Co., Ltd., Seoul, Republic of Korea) followed by analysis of the left cheek with Image-Pro 10 (Media Cybernetics, Inc., Rockville, MD, USA); it was defined as the angle formed where a horizontal line originating at the tip of the nose meets a contour derived from the nasolabial fold, such that a decrease in the angle indicates a lifting effect. Dermal density (dermal echodensity by high-frequency ultrasound) was measured at the right cheek with the Ultrascan UC22 (Courage + Khazaka electronic GmbH, Cologne, Germany).

The barrier category comprised a single indicator, transepidermal water loss (TEWL), measured at the right cheek with the Tewameter TM HEX (Courage + Khazaka electronic GmbH, Cologne, Germany), an open-chamber device reporting water loss in grams per square meter per hour (g/m^2/h).

The complexion category comprised three indicators. Skin roughness (a texture index based on three-dimensional surface mapping) was measured at the left cheek with the Antera 3D CS in Texture mode. Skin radiance, which corresponds to the skin-quality attribute of skin glow, was quantified as skin gloss measured at the right cheek with the SkinGlossMeter (Delfin Technologies Ltd., Kuopio, Finland); clinical facial images were also taken in Parallel mode with the VISIA-CR (Canfield Scientific, Inc., Parsippany, NJ, USA) for documentation. Skin tone (the L* value) was obtained by frontal facial imaging in Standard mode with the VISIA-CR followed by analysis of the right cheek with Image-Pro 10. For this analysis, a region of interest of 500 × 500 pixels was placed within the cheek; its position was set for each participant according to the shape of the face and the characteristics of the cheek, and the same position was used for that participant at every visit.

The dark-circle category comprised three indicators. Dark-circle brightness (the L* value) was measured at the right infraorbital region with the Spectrophotometer CM-700d (Konica Minolta, Inc., Tokyo, Japan), and the dark-circle melanin index was measured at the same right infraorbital site with the Mexameter MX 18 (Courage + Khazaka electronic GmbH, Cologne, Germany). The dark-circle grade was obtained by visual evaluation of the VISIA-CR images by two evaluators, each with at least five years of experience in dermatological clinical testing, on a 0-to-5 ordinal grading scale, in which the grade was assigned according to the extent of purplish shadowing and pigmentation of the infraorbital region. Grades were defined as follows: 0, no perceptible dark circle; 1, a faint violet shadow at the medial lower eyelid that darkens when the skin is stretched; 2, a violet shadow clearly visible without stretching, faint pigmentation, or both; 3, a deep violet shadow, moderate pigmentation over part of the area, or both; 4, uniform dense pigmentation across the area, often extending to the upper as well as the lower eyelid; 5, uniform and very dense pigmentation involving both the upper and the lower eyelid. For each participant and time point, the higher of the two grades was adopted for the analysis. The two evaluators assigned the same grade in 60 of the 66 paired ratings (22 participants at three time points; 90.9%), all six discordant pairs differed by a single grade, and agreement was Cohen's $\kappa = 0.82$ (linear-weighted $\kappa = 0.83$), with complete agreement at baseline.

The last application before the week-2 and week-4 visits was made on the preceding evening, and the measurements were made the following day. The Cutometer dual MPA580 was used with a 2 mm probe at 450 mbar and three suction cycles of 2 s on and 2 s off; the Tewameter TM HEX probe, with an opening of approximately 1 cm, was held on the site for at least 20 s until the reading stabilized; the Spectrophotometer CM-700d was used in SCI mode with a 3 mm aperture, a D65 illuminant and a 10° observer; the Mexameter MX 18 used a 5 mm probe; and the SkinGlossMeter directed a 635 nm red semiconductor laser onto a spot 50 μm in diameter and detected the light reflected at the angle equal to the angle of incidence, that is, the specular component, as distinct from the light scattered at the skin surface and within the tissue. The detected light passed through an internal diffractive microstructure, and its intensity was converted into a gloss reading in skin gloss units (SGU), an instrument-specific unit that, according to the manufacturer, is derived from the industrial gloss unit and scaled for the low gloss values of skin; a higher value indicates a glossier surface. The Antera 3D CS captured a 56 × 56 mm field. For the Cutometer, Tewameter, Mexameter, Spectrophotometer and SkinGlossMeter, three consecutive readings were taken at the same site and averaged, with a predefined tolerance applied to the spread of the three readings; the Antera 3D CS and the VISIA-CR were recorded once per visit. Measurement sites were relocated at each visit from fixed anatomical landmarks: for the probe measurements on the cheek, the point on the cheek defined by the center of the eye and the tip of the nose; for the infraorbital measurements, the region below the medial canthus; and for the Antera 3D CS, the periorbital region for eye wrinkles and the center of the cheek for skin volume and roughness. For the VISIA-CR, the head was held in a chin rest at a fixed position and each new capture was aligned to the previous image by overlay. The mean within-subject coefficient of variation in the triplicate readings, computed over 66 replicate sets per instrument (22 participants at three time points), was 0.43% for the Mexameter MX 18, 0.50% for the Spectrophotometer CM-700d, 0.74% for the Tewameter TM HEX, 0.94% and 1.40% for the Cutometer dual MPA580 (R2 and R7), and 2.08% for the SkinGlossMeter. These coefficients of variation refer to readings taken at a single site within one visit; the error introduced by relocating the site between visits was not quantified.

With respect to the direction of change, the direction corresponding to improvement was defined for each indicator. Measured values for which a decrease indicates improvement were eye wrinkles, lifting angle, TEWL, skin roughness, dark-circle melanin, and

dark-circle grade (6 indicators); for the remaining 7 indicators, an increase indicates improvement.

Wellness indicators. The three wellness indicators were assessed before use and at week 4. Sleep duration was measured in minutes using a wearable device (Fitbit Charge 5; Fitbit LLC, San Francisco, CA, USA). A 7-day period before product use served as the baseline phase, and a period of at least 1 week measured 21 to 28 days after the start of product use served as the post-treatment phase; daily sleep-duration values from both phases were used. Sleep varies considerably from night to night, so a single night does not give a stable estimate of habitual sleep duration and multiple nights were averaged. Seven consecutive nights were used in each phase so that a full week, including both weekday and weekend nights, was covered [47]. The post-treatment window was placed in the final week of the 4-week application period (days 21 to 28) so that it reflects sleep during treatment closest to the 4-week endpoint. A total of 306 nights contributed to the analysis: 154 nights in the baseline phase, comprising 7 nights for each of the 22 participants, and 152 nights in the post-treatment phase, comprising 7 nights in 20 participants and 6 nights in the remaining 2. For each participant, a mean sleep duration was computed for each phase without imputation of missing nights, and these participant-level means were entered into the paired analysis. Sleep quality was assessed with the PSQI-K, and mood was assessed with the Patient Health Questionnaire-9 (PHQ-9) [48]. For the PSQI-K and PHQ-9, a decrease in score indicates improvement, whereas for sleep duration an increase indicates improvement.

Salivary biomarkers. Salivary samples were collected in the daytime and at night, before use and at week 4. The daytime sample was obtained on site on the day of the visit at 12:00 or 14:00, at the same time for each participant at baseline and at week 4, and the nighttime sample was self-collected at home on the preceding evening, approximately 2 h before bedtime, under dim lighting. No allowable nighttime collection window was prespecified. Completion of the home nighttime collection was confirmed by message, but actual collection times were not recorded. Participants refrained from toothbrushing and from any oral intake during the 30 min preceding collection, and immediately before collection they gently massaged the submandibular region to stimulate salivary flow; saliva was then collected by passive drool through a funnel into the collection tube. The massage was used to facilitate sufficient sample volume; salivary gland massage has been reported to increase salivary flow [49]. Because stimulation during collection can affect the measured concentrations of salivary steroids [50], the same procedure was used at baseline and at week 4 for every participant. All biomarker assays were performed by a specialized analytical laboratory (LABISKOMA, Seoul, Republic of Korea).

Saliva samples were stored at −80 °C until analysis and thawed once, immediately before the assays; each sample was then centrifuged at 10,000× *g* for 4 min at 4 °C, and the resulting supernatant was used for the assays. Two analytes were quantified by commercial colorimetric enzyme-linked immunosorbent assays (ELISAs): melatonin with the Melatonin ELISA kit (ab283258; Abcam, Cambridge, UK) and cortisol with the Human Cortisol ELISA Kit (KA1885; Novus Biologicals, Centennial, CO, USA). Each of the two analytes was assayed with its respective kit in the paired daytime and nighttime samples, yielding four directly measured concentrations (daytime and nighttime melatonin, and daytime and nighttime cortisol). All assays were performed according to the manufacturers' protocols. The calibration range was 1–64 pg/mL for melatonin and 0.1–30 ng/mL for cortisol, the analytical sensitivity was 0.6 pg/mL and 0.019 ng/mL, respectively, and the intra- and inter-assay coefficients of variation were 4.8–5.1% and 8.3–11.1% for melatonin and 4.1–7.1% and 4.2–9.1% for cortisol. To normalize for sample-to-sample differences in total protein, the total protein concentration of each sample was determined by a bicinchoninic acid (BCA) assay (absorbance at 562 nm; Thermo Fisher Scientific, Waltham, MA, USA),

and biomarker concentrations were expressed per milligram of protein (melatonin, pg/mg protein; cortisol, ng/mg protein). The same normalization, with total protein determined by a BCA assay, has been applied to salivary melatonin and cortisol in a study of circadian biomarkers [51].

The two day–night difference measures were derived from these values as signed differences between the daytime and nighttime concentrations: the melatonin day–night difference was calculated as night minus day (reflecting normal nighttime dominance), and the cortisol day–night difference was calculated as day minus night (reflecting normal daytime dominance). Together with the four measured concentrations, these two derived indices constituted the six before-and-after comparisons evaluated in the salivary biomarker domain. The direction of improvement followed the day–night pattern expected physiologically for each hormone: a decrease denotes improvement for daytime melatonin and nighttime cortisol, and an increase denotes improvement for nighttime melatonin, daytime cortisol, and the two day–night differences.

2.3.5. Safety Evaluation

Adverse skin reactions were assessed after 2 and 4 weeks of product use. At each assessment the investigator examined the application area, and each participant was separately asked to report her own experience during the preceding period of use; together, the two routes covered erythema, edema, scaling, itching, stinging, burning, tightness, and prickling, as well as any other adverse reaction.

2.3.6. Statistical Analysis

All analyses were performed in Python 3.14.1 with the pandas (version 3.0.0), NumPy (version 2.4.2), and SciPy (version 1.17.0) libraries; the figures presenting the study data were generated with Matplotlib (version 3.10.8) and seaborn (version 0.13.2).

Statistical tests were performed on the measured values as recorded. For indicators in which a decrease in the measured value represents clinical improvement, the sign was reversed when the effect size, the Hodges–Lehmann change estimate and its confidence interval, the relative change from baseline (%), and the proportion of participants with a change in the defined direction were computed, so that a positive value denotes improvement across all indicators.

Each skin indicator was compared between baseline and week 2 and between baseline and week 4, and each wellness indicator between baseline and week 4. All of these within-participant comparisons were analyzed with the two-sided Wilcoxon signed-rank test. A rank-based test was applied consistently to every paired comparison because the appropriateness of distributional assumptions cannot be assessed reliably in a sample of this size and because the outcome measures comprised both continuous and ordinal variables. In each comparison, pairs with a difference of exactly zero were excluded from the test; for an ordinal indicator on which many participants show no change between visits, this reduces the number of pairs entering the comparison below the number of participants, and the number actually used is reported with the corresponding result. For each comparison the change was also summarized by the Hodges–Lehmann estimate, the median of the Walsh averages of the within-participant differences, with a two-sided 95% confidence interval derived from the exact null distribution of the signed-rank statistic. Unlike the test, the estimate and the interval were computed from all pairs, including those with a difference of zero, so that they describe the change in the cohort as a whole, and they carry no correction for multiple comparisons. Relative change from baseline (%) was calculated as $(\text{mean}_{\text{after}} - \text{mean}_{\text{before}})/\text{mean}_{\text{before}} \times 100$.

Effect sizes were expressed as Cohen's d, a descriptive measure of the standardized mean change in a paired design, in which the within-subject change is standardized by

the pooled pre- and post-treatment standard deviation: d = mean(post − pre)/√[(SD_{before}^2 + SD_{after}^2)/2]. Standardized mean changes for paired designs may be expressed with several denominators, and the pooled standard deviation was used consistently here [52]. Values of approximately 0.2, 0.5, and 0.8 were used to characterize standardized changes as small, medium, and large, respectively; these labels are descriptive only and do not denote clinical importance [53]. The dark-circle grade is recorded as a 0-to-5 ordinal grade, with a difference between visits of either one grade or none. Cohen's d was computed for it with the same formula as for the other indicators, which treats the grades as equally spaced and therefore standardizes the mean change in grade rather than estimating a quantity on the scale.

Multiple comparisons were corrected with the Benjamini–Hochberg (BH) procedure. For the clinical outcomes, the BH-adjusted value is denoted p_{adj} and the uncorrected value the raw p-value; the dose–response comparisons in vitro are reported as the Dunnett-adjusted values described above and are denoted p, whereas the two-condition knockdown comparisons are reported as unadjusted two-tailed values; statistical significance was defined as p_{adj} below 0.05, and the significance markers in the clinical figures likewise refer to p_{adj}. Supplementary Tables S2 to S4 report, for each comparison, the median and interquartile range before and after treatment, the Hodges–Lehmann change with its confidence interval, Cohen's d, and the raw and adjusted p-values side by side, so that the magnitude and the statistical strength of each change can be assessed together.

Correction was applied within each outcome domain, because the three domains address distinct hypotheses. Each family comprised the before-versus-after comparisons of that domain: the 13 skin indicators at the 2 post-treatment time points (26 tests), the 3 wellness indicators at week 4 (3 tests), and the 4 measured biomarker concentrations together with the 2 derived day–night differences at week 4 (6 tests). Melatonin and cortisol were placed in a single biomarker family on mechanistic grounds: melatonin is an output hormone of the circadian system and cortisol is a product of the hypothalamic–pituitary–adrenal axis, so that the two hormones and the day–night differences derived from them address the same hypothesis about the diurnal output of these two coupled axes.

Each of the six before-and-after comparisons in the salivary biomarker domain was made between baseline and week 4 with the same Wilcoxon signed-rank test. To examine the influence of high baseline melatonin concentrations, baseline daytime and nighttime values above the upper Tukey fence—the third quartile plus k times the interquartile range of the 22 baseline values at that time of day, with k = 3.0 and k = 1.5—were set to the fence value. No observation was removed; the six biomarker comparisons were re-tested on the capped values and the BH correction was reapplied. The same six comparisons were also repeated on the unnormalized concentrations, with the BH correction applied across those six comparisons; both sets are reported in Supplementary Table S4.

3. Results

3.1. In Vitro Assays: PER2 Promoter-Driven Luciferase Output and Inflammatory Transcripts

PER2 is a core clock gene of the peripheral cutaneous clock. A *PER2* promoter–luciferase reporter assay was performed in HaCaT keratinocytes to measure the effect of the six-botanical mixture extract on *PER2* promoter-driven luciferase output: the cells were synchronized with dexamethasone and treated for 24 h, the medium was then exchanged for recording medium, and bioluminescence was followed hourly for 72 h. The reporter oscillated over the recording period (Figure 2a,c). Peak bioluminescence rose with the concentration of the mixture extract in each of the three circadian cycles resolved within the recording, reaching 3.79-, 3.03-, and 2.70-fold of the DMSO control at 50 µg/mL (linear contrast across concentrations, $p < 0.001$ in every cycle; Figure 2b), and the amplitude of the rhythm rose in parallel (linear contrast, $p < 0.001$; Figure 2d; Supplementary Table S1).

Cell viability did not differ across concentrations ($p = 0.486$), so these changes are not attributable to differences in the number or metabolic state of the cells. Together these results indicate that the mixture extract raises *PER2* promoter-driven luciferase output in keratinocytes. In a separate reverse-transcription quantitative PCR experiment, endogenous *PER2* mRNA rose with the concentration of the mixture extract at both 24 h and 48 h (linear contrast, $p = 0.010$ and $p = 0.006$; Figure 2e; Supplementary Table S1).

The cutaneous clock is known to regulate epidermal inflammatory signaling [17,19], and IL-6 and CXCL-10 are representative keratinocyte pro-inflammatory mediators. To test whether PER2 governs this local inflammatory node in keratinocytes, *PER2* was knocked down with a *PER2*-targeting siRNA, which lowered *PER2* transcript levels and increased *IL6* and *CXCL10* expression (Figure 3). Building on this, treatment with the mixture extract reduced the expression of the same two transcripts relative to the vehicle control (Figure 4a,b). Taken together, in keratinocytes the mixture extract raised *PER2* promoter-driven luciferase output and reduced the expression of *IL6* and *CXCL10*, two PER2-associated inflammatory mediators.

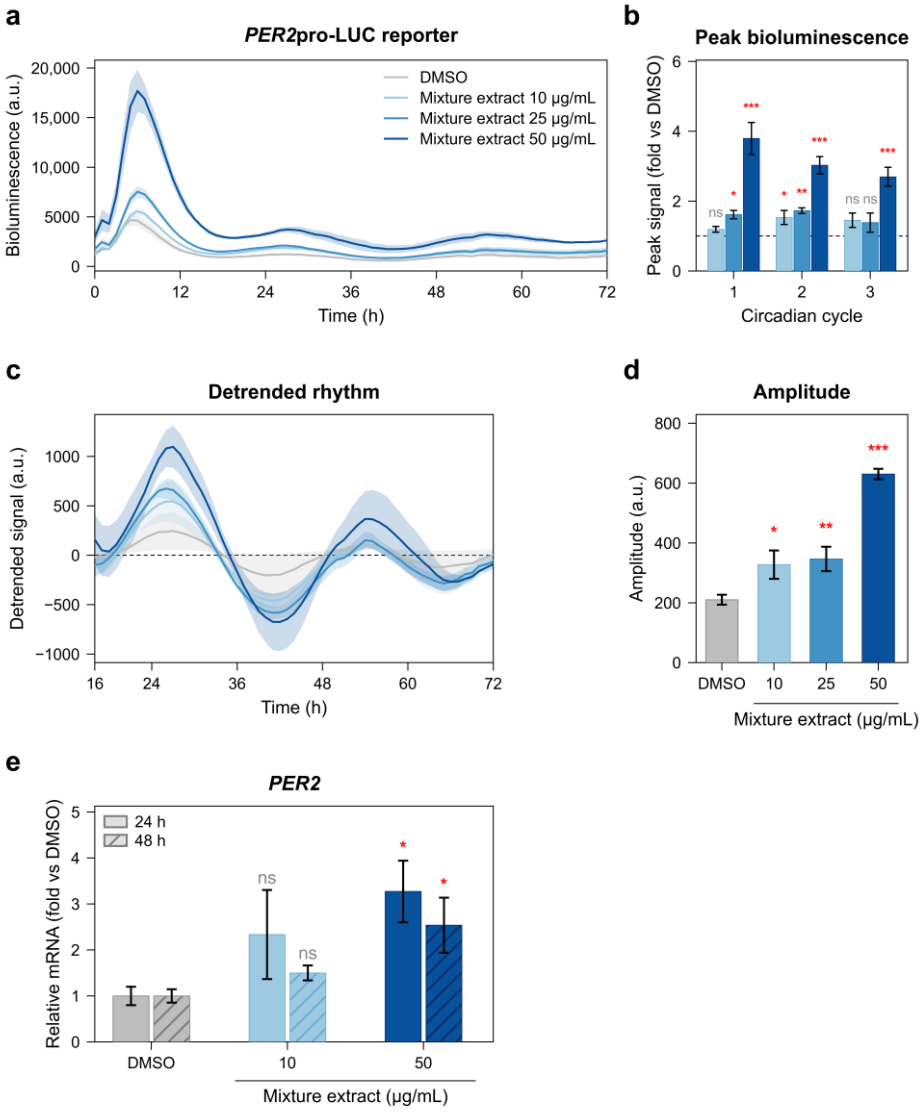


Figure 2. *PER2* promoter-driven luciferase output, rhythm amplitude, and endogenous *PER2* mRNA in HaCaT keratinocytes treated with the six-botanical mixture extract ($n = 3$ per group). In all panels, gray denotes the vehicle (DMSO) control and progressively darker blue denotes the mixture extract at 10, 25, and 50 µg/mL, as indicated in (a); in (e), hatched bars denote the 48 h exposure.

(**a**) *PER2* promoter–luciferase (PER2pro-LUC) reporter assay in HaCaT cells treated with vehicle (DMSO) or the mixture extract at 10, 25, or 50 µg/mL: bioluminescence traces recorded hourly over 0 to 72 h; lines denote the group mean and shaded bands the SD. (**b**) Peak bioluminescence of each of the three circadian cycles resolved within the recording, taken as the maximum of the trace within 0 to 18 h, 18 to 40 h, and 42 to 68 h and expressed relative to the DMSO control of the same cycle; the dashed line marks the DMSO control, bars denote the mean and error bars the SD. (**c**) The records in (**a**) after subtraction of a 24 h moving average and smoothing with a 3 h moving average, shown over the 16 to 72 h interval used for rhythm analysis; lines denote the group mean, shaded bands the SD, and the dashed line the zero level. (**d**) Amplitude of the rhythm in arbitrary units, obtained from the records in (**c**) by the fast Fourier transform–nonlinear least squares method; bars denote the mean and error bars the SD. (**e**) Endogenous *PER2* mRNA in HaCaT cells treated with vehicle (DMSO) or the mixture extract at 10 or 50 µg/mL for 24 h or 48 h, normalized to the reference gene *PUM1* and expressed relative to the DMSO control of the same experiment, which is therefore set to 1; bars denote the mean and error bars the SD. All groups comprise $n = 3$ independent experiments. In (**b**) and (**d**), matched treatment conditions were compared by one-way repeated-measures analysis of variance (ANOVA) followed by Dunnett's multiple-comparisons test comparing each concentration with the DMSO control, with the independent experimental run treated as the blocking factor, and concentration dependence was tested by a linear contrast across the four concentrations (see Methods); each cycle in (**b**) was analyzed as a separate family. In (**e**), the same model was applied separately at each exposure time, with the linear contrast taken across the three concentrations. *** $p < 0.001$, ** $p < 0.01$, * $p < 0.05$, ns = not significant.

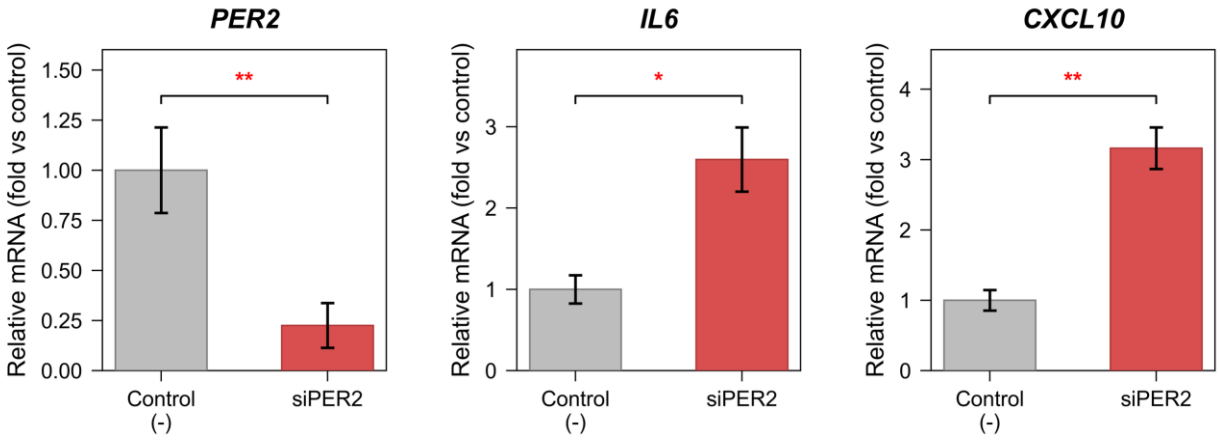


Figure 3. *PER2* knockdown and inflammatory transcript levels in HaCaT keratinocytes. *PER2*, *IL6*, and *CXCL10* mRNA expression in HaCaT keratinocytes transfected with a non-targeting control siRNA [Control (-)] or a *PER2*-targeting siRNA (siPER2) ($n = 3$ independent experiments per group). Expression was normalized to the reference gene *PUM1* and is expressed relative to Control (-), which is therefore set to 1; bars denote the mean and error bars the SD. Control (-) and siPER2 were compared by a two-tailed paired t test. ** $p < 0.01$, * $p < 0.05$.

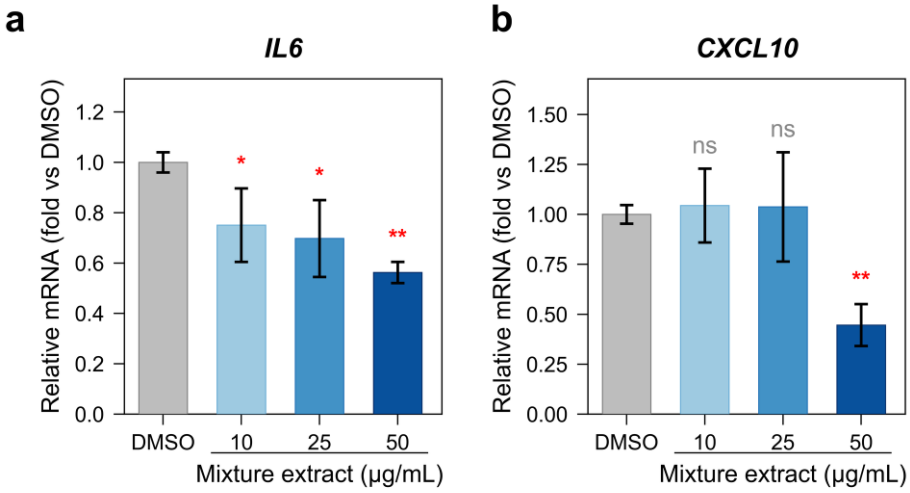


Figure 4. *IL6* and *CXCL10* expression in HaCaT keratinocytes treated with the six-botanical mixture extract ($n = 3$ per group). (**a**,**b**) *IL6* (**a**) and *CXCL10* (**b**) mRNA expression in cells treated with vehicle (DMSO) or the mixture extract at 10, 25, or 50 µg/mL for 24 h. Expression was normalized to the reference gene *PUM1* and is expressed relative to the DMSO control, which is therefore set to 1; bars denote the mean and error bars the SD. All groups comprise $n = 3$ independent experiments. Matched treatment conditions were compared by one-way repeated-measures analysis of variance (ANOVA) followed by Dunnett's multiple-comparisons test comparing each concentration with the DMSO control, with the independent experimental run treated as the blocking factor. ** $p < 0.01$, * $p < 0.05$, ns = not significant.

3.2. Skin Indicators Across the Four Functional Categories

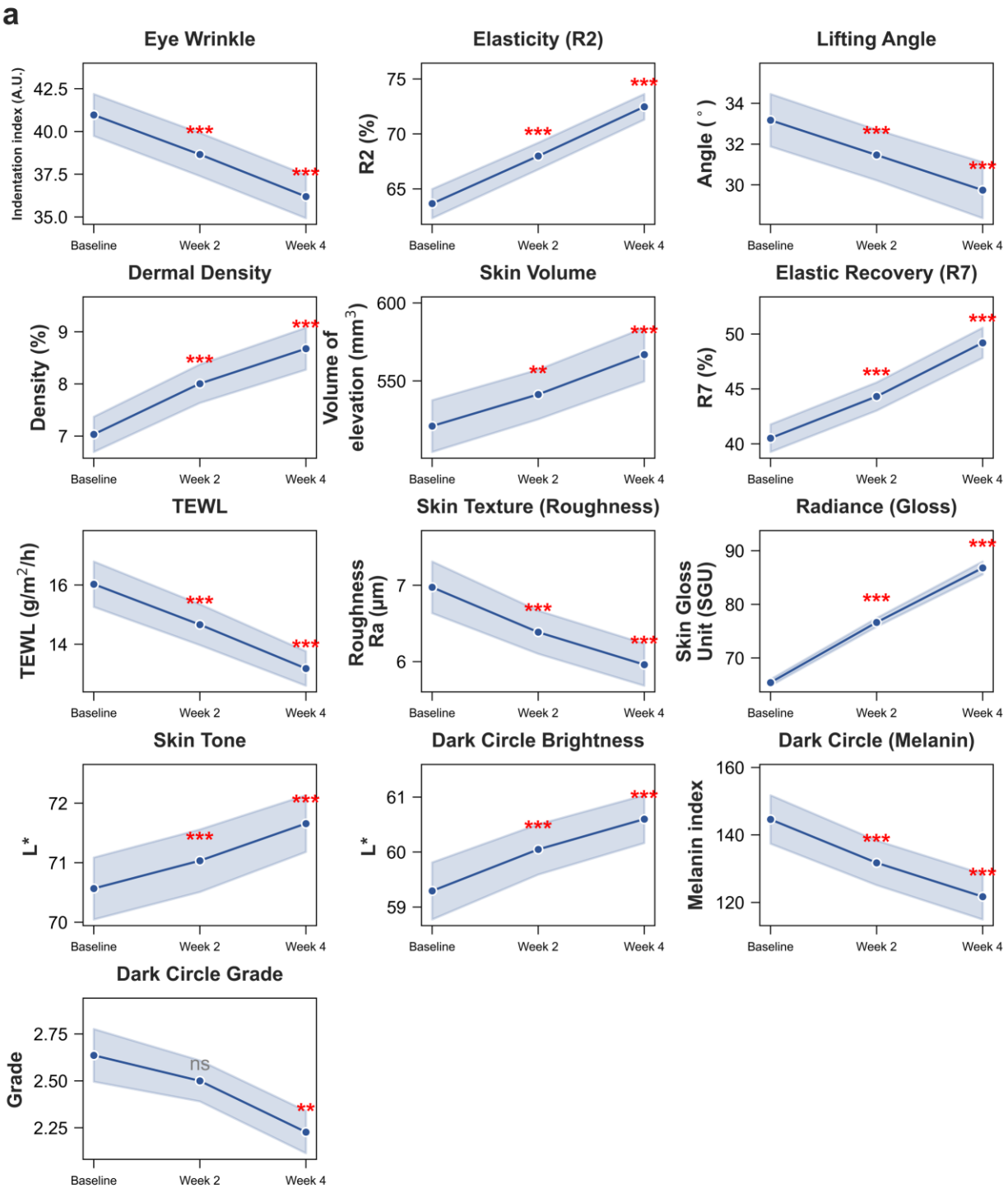
Following the in vitro characterization of the mixture extract, the test cream was applied for 4 weeks in the cohort (N = 22) and the 13 skin indicators were evaluated. Every one of the 13 skin indicators changed significantly from baseline at week 4 (Wilcoxon signed-rank test; all $p_{adj} < 0.05$, and 12 of the 13 at $p_{adj} < 0.001$), with Cohen's d spanning 0.47 to 4.81 (Figure 5a,b; Supplementary Table S2). These changes are described below according to the four functional categories; clinical images of skin texture and dark circles, each from two participants, are shown in Figure 5c.

The six anti-aging indicators all changed significantly from baseline at week 4. The largest of these changes were in dermal density, which increased by 23.37% ($d = 0.94$, $p_{adj} < 0.001$), and elastic recovery (R7), which increased by 21.41% ($d = 1.41$, $p_{adj} < 0.001$); skin elasticity (R2) increased by 13.83% ($d = 1.51$, $p_{adj} < 0.001$), the strongest effect size in the category. The remaining three indicators also changed significantly: eye wrinkles decreased by 11.65% ($d = 0.82$, $p_{adj} < 0.001$), the skin lifting angle decreased by 10.35% ($d = 0.55$, $p_{adj} < 0.001$, a decrease in the measured value denoting a lifting effect), and skin volume increased by 8.81% ($d = 0.58$, $p_{adj} < 0.001$). At week 4, the proportion of participants whose value changed in the defined direction was 100% or 95.5% (21 of 22) for every one of the six indicators.

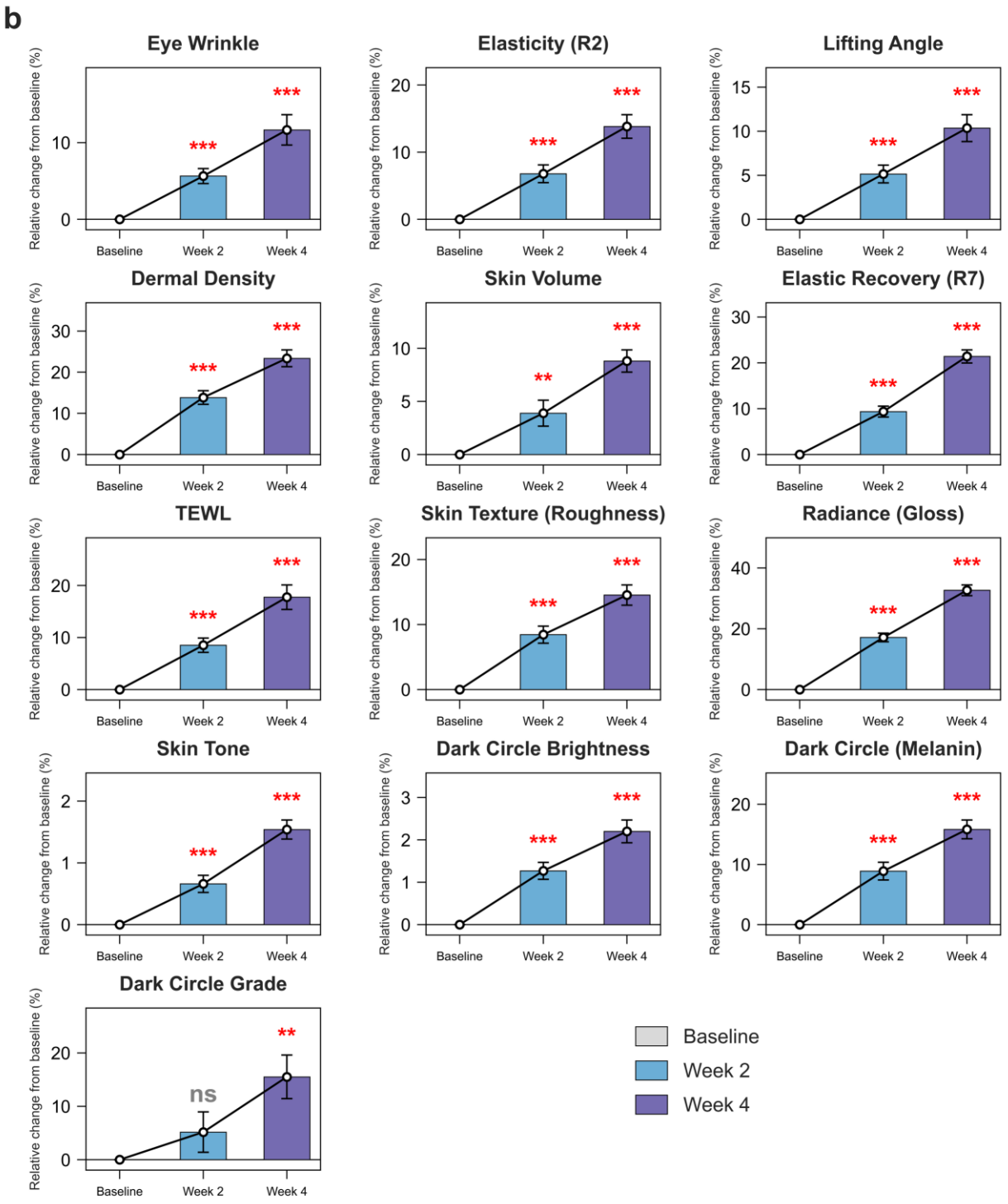
The barrier category comprised a single indicator, transepidermal water loss (TEWL), which decreased by 17.76% ($d = 0.89$, $p_{adj} < 0.001$), with a decrease observed in all 22 participants. This reduction was consistent across participants.

Within the complexion category, skin roughness decreased by 14.53% ($d = 0.70$, $p_{adj} < 0.001$), skin radiance increased by 32.65% ($d = 4.81$, $p_{adj} < 0.001$, the largest effect size in the study), and skin tone (L*) increased by 1.54% ($d = 0.47$, $p_{adj} < 0.001$). All three indicators changed in the defined direction in all 22 participants. The large effect size for skin radiance arose because its mean change (21.36 units) was large relative to the pooled pre- and

post-treatment standard deviation (4.45), rather than because of an unusually small denominator.



https://doi.org/10.3390/cosmetics13060301



https://doi.org/10.3390/cosmetics13060301

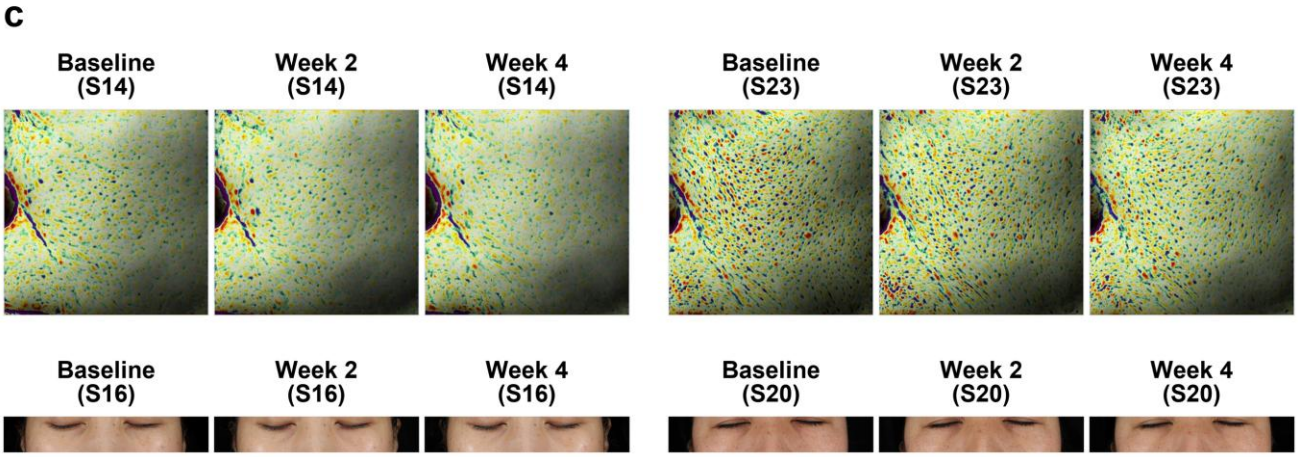


Figure 5. Time course of the 13 skin indicators over 4 weeks of once-nightly application of the test cream (N = 22). (**a**) Measured values at baseline, week 2, and week 4 for each indicator, presented in four functional categories: anti-aging (eye wrinkle, elasticity [R2], lifting angle, dermal density, skin volume, elastic recovery [R7]), barrier (transepidermal water loss [TEWL]), complexion (skin texture [roughness], radiance [gloss], skin tone [L*]), and dark circle (brightness [L*], melanin, grade). Symbols denote the group mean at each time point and the shaded band the standard error of the mean (SEM); the band therefore indicates the precision of that mean rather than the spread of the individual values. The *y*-axis of each panel is scaled in the measurement unit of that indicator. (**b**) Relative change from baseline (%) at the same time points for the same 13 indicators, expressed as a percentage of the baseline mean. For the six indicators in which a decrease in the measured value denotes improvement (eye wrinkle, lifting angle, TEWL, skin texture, dark-circle melanin, and dark-circle grade), the sign was reversed, so that a positive value denotes improvement for every indicator. The horizontal line marks 0% (no change from baseline). Bars give the mean relative change at each time point, and the open circle on each bar marks the same value and is joined by a line to show the time course. Error bars denote the SEM of the relative change, obtained by expressing the SEM of the within-participant change (Δ) as a percentage of the baseline mean; this SEM therefore describes the within-participant change, whereas the band in (**a**) describes the group mean at a single time point. (**c**) Clinical images at baseline, week 2, and week 4. Upper row, skin texture in participants S14 and S23 (Antera 3D CS); lower row, dark circles in participants S16 and S20 (VISIA-CR). Each pre-versus-post comparison was tested by the two-sided Wilcoxon signed-rank test, and multiple comparisons were corrected by the Benjamini–Hochberg procedure. Significance markers denote the adjusted *p*-value (p_{adj}) for the comparison against baseline at the indicated time point. *** $p_{adj} < 0.001$, ** $p_{adj} < 0.01$, ns = not significant.

Within the dark-circle category, dark-circle brightness (L*) increased by 2.20% (d = 0.58, $p_{adj} < 0.001$) and the dark-circle melanin index decreased by 15.82% (d = 0.70, $p_{adj} < 0.001$), with brightness increasing and melanin decreasing in all 22 participants. The dark-circle grade, based on visual evaluation of the images by the two trained evaluators, exhibited a time-dependent pattern: it was not significant at week 2 (raw p = 0.180, p_{adj} = 0.180) but reached significance at week 4, when it decreased by 15.52% (d = 0.69, p_{adj} = 0.003), with a decrease in 9 of the 22 participants (40.9%). This grade is an ordinal scale on which many participants showed no change between visits, and because the Wilcoxon signed-rank test excludes pairs with a zero difference, the comparison rested on 5 informative pairs at week 2 and on 9 at week 4, whereas every other indicator used all 22 pairs. The optical and pigmentary measures therefore reached significance before the visual grading did.

With respect to the time course, 12 of the 13 indicators had already changed significantly from baseline at week 2 ($p_{adj} < 0.05$), and the effect size at week 4 was numerically

larger than the effect size at week 2 for every one of the 13 indicators. The dark-circle grade was the only indicator that was not significant at week 2 and significant at week 4.

3.3. Wellness Indicators: Sleep Duration, Sleep Quality, and Mood

On the basis of a bidirectional sleep–skin axis hypothesis, three wellness indicators were evaluated. All three changed significantly from baseline at week 4 (Figure 6; Supplementary Table S3).

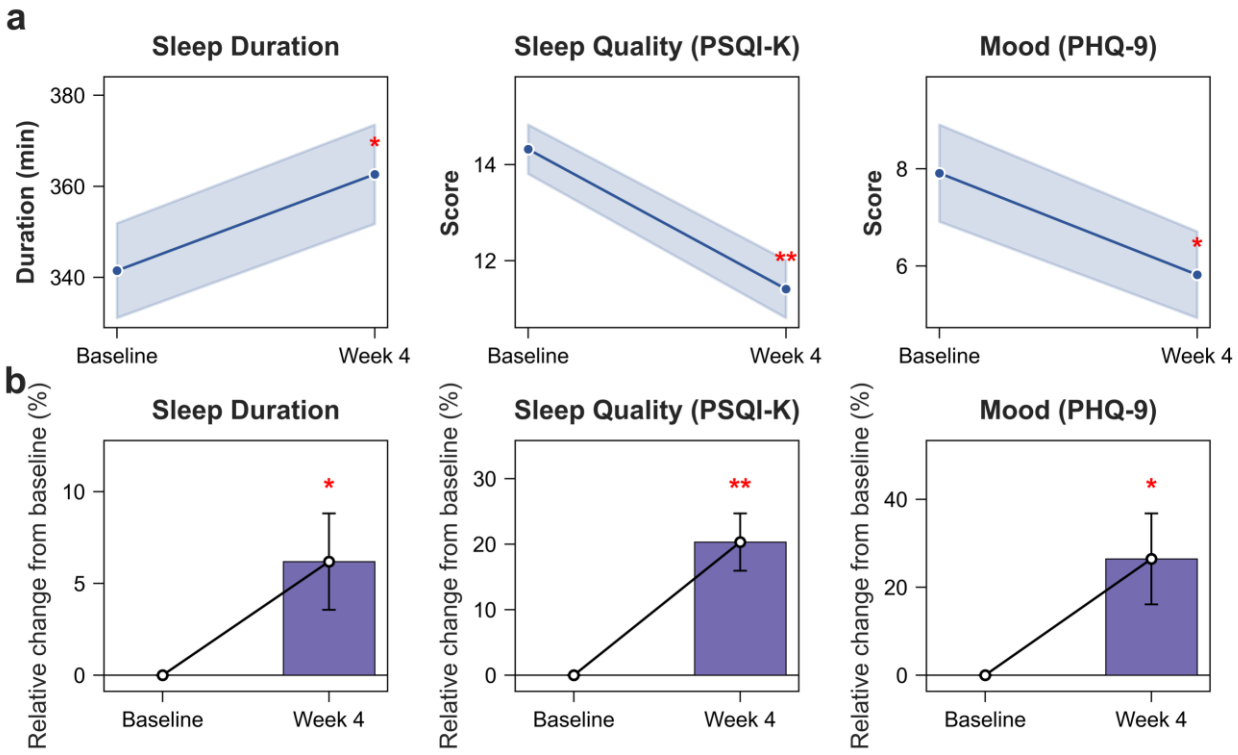


Figure 6. Wellness indicators before and after 4 weeks of once-nightly application of the test cream (N = 22). (**a**) Measured values at baseline and week 4 for sleep duration (min, recorded with a wearable device), sleep quality (PSQI-K score), and mood (PHQ-9 score). Symbols denote the group mean and the shaded band the SEM. (**b**) Relative change from baseline (%) for the same three indicators, expressed as a percentage of the baseline mean. As in Figure 5b, the sign was reversed for the two indicators in which a decrease in score denotes improvement (PSQI-K and PHQ-9), so that a positive value denotes improvement for every indicator. The horizontal line marks 0% (no change from baseline). Purple bars give the mean relative change at week 4, the open circle on each bar marks the same value and is joined by a line, and the error bars denote the SEM of the relative change, obtained by expressing the SEM of the within-participant change (Δ) as a percentage of the baseline mean, as in Figure 5b. Each comparison was tested by the two-sided Wilcoxon signed-rank test, and multiple comparisons were corrected by the Benjamini–Hochberg procedure; the significance markers denote the adjusted *p*-value (p_{adj}). ** $p_{adj} < 0.01$, * $p_{adj} < 0.05$.

Sleep duration, measured with a wearable device (Fitbit Charge 5), increased by 6.19% (from a baseline mean of 341.49 min to 362.63 min at week 4; $d = 0.42$; raw $p = 0.021$, $p_{adj} = 0.021$), with an increase observed in 16 of 22 participants (72.7%). The sleep quality score (PSQI-K) decreased by 20.32% (from a baseline mean of 14.32 to 11.41 at week 4, a lower score denoting better sleep quality; $d = 1.11$; raw $p < 0.001$, $p_{adj} = 0.001$), with a decrease in 17 of 22 participants (77.3%); this was the largest effect size among the wellness indicators. The mood score (PHQ-9) decreased by 26.44% (from a baseline mean of 7.91 to 5.82 at week 4, a lower score denoting better mood; $d = 0.47$; raw $p = 0.012$, $p_{adj} = 0.018$),

with a decrease in 14 of 22 participants (63.6%). However, because sleep duration was averaged over days 21 to 28 to reduce night-to-night variability, whereas the skin and salivary measures were obtained at the week-4 visit, these outcomes represent closely aligned but not identical assessment windows.

All three indicators changed significantly at the group-mean level over the 4-week application period, although the change was less uniform across participants than in the skin domain.

3.4. Salivary Biomarkers: Day–Night Differences in Melatonin and Cortisol

Melatonin and cortisol are representative circadian outputs related to the sleep–wake cycle and the hypothalamic–pituitary–adrenal axis, respectively. To explore, on the basis of the same sleep–skin axis hypothesis, whether melatonin and cortisol, the hormonal measures related to sleep and affective state, changed during use of the test cream, daytime and nighttime concentrations of the two hormones and their day–night differences were evaluated before and after use (Figure 7). Because the distribution of each hormone was skewed by a few high values, concentrations are summarized here as medians, with the means, standard deviations, and interquartile ranges given in Supplementary Table S4.

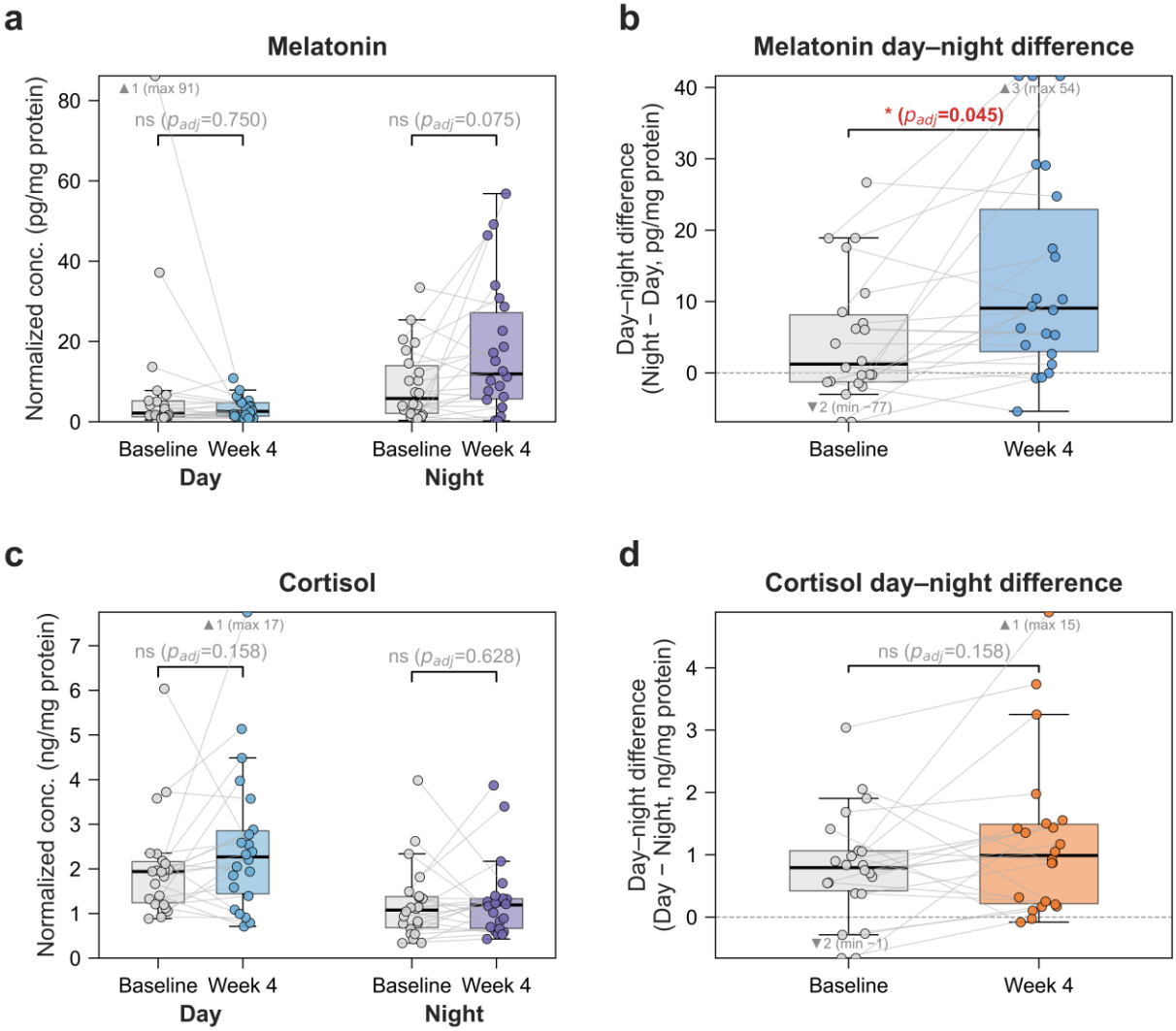


Figure 7. Salivary biomarkers before and after 4 weeks of once-nightly application of the test cream (N = 22). (**a**–**d**) Before-and-after comparison of melatonin (**a**), the melatonin day–night difference

(**b**), cortisol (**c**), and the cortisol day–night difference (**d**). Melatonin and cortisol were each measured separately in daytime and nighttime samples; the day–night difference is the signed night-minus-day contrast for melatonin and the signed day-minus-night contrast for cortisol. All concentrations are normalized to the total protein content of the sample (melatonin, pg/mg protein; cortisol, ng/mg protein). Boxes denote the median and interquartile range, and whiskers extend to 1.5 times the interquartile range. Overlaid points are the individual values of the 22 participants, and the gray lines connect the paired baseline and week 4 values of the same participant. In (**b**) and (**d**), the dashed horizontal line marks zero, the boundary between the normal orientation of the contrast and an inverted one; a positive value denotes the physiologically normal orientation (nighttime-dominant for melatonin, daytime-dominant for cortisol). For readability, the *y*-axis of each panel is limited to the range spanned by the bulk of the pooled data rather than by its extremes; values falling outside the axis are not lost but are indicated at the axis edge by the annotation ▲n or ▼n, which gives the number of such values together with the most extreme one. Baseline-versus-week 4 comparisons were tested by the two-sided Wilcoxon signed-rank test, and multiple comparisons were corrected by the Benjamini–Hochberg procedure; the adjusted *p*-value (p_{adj}) is printed above each bracket. * $p_{adj} < 0.05$, ns = not significant.

The nighttime-dominant melatonin day–night difference (night minus day) increased from a median of 1.227 to 9.068 pg/mg protein and was significant ($d = 0.75$; raw $p = 0.007$, $p_{adj} = 0.045$), with an increase in 14 of the 22 participants (Figure 7a,b). Daytime melatonin did not change significantly, moving from a median of 2.189 to 2.611 pg/mg protein, with a change in the defined direction in 11 of the 22 participants ($d = 0.38$; raw $p = 0.750$, $p_{adj} = 0.750$). Nighttime melatonin increased from a median of 5.807 to 11.931 pg/mg protein, with an increase in 15 of the 22 participants; this change was significant before correction but not after it ($d = 0.64$; raw $p = 0.025$, $p_{adj} = 0.075$). The widening of the day–night difference therefore rested on the nighttime concentration, and statistical significance was reached in the derived difference rather than in either concentration on its own.

Melatonin concentrations differed widely between participants, and a few had markedly high values at baseline. To examine whether those values accounted for the change in the day–night difference, baseline daytime and nighttime concentrations above the upper Tukey fence were set to the fence value and the comparison was repeated (Supplementary Table S5). The day–night difference still increased from baseline in 14 of the 22 participants and Cohen's *d* changed little (0.73 and 0.70 with $k = 3.0$ and $k = 1.5$, against 0.75). However, the Hodges–Lehmann estimate of the change decreased from 10.181 pg/mg protein in the primary analysis to 6.281 and 5.214 pg/mg protein, with unadjusted 95% confidence intervals that excluded zero in all three analyses, and the comparison gave raw $p = 0.007$ and 0.009 and $p_{adj} = 0.045$ and 0.056, respectively. No participant was excluded on the basis of a high baseline value. The amount of salivary melatonin secreted has been reported to differ by more than an order of magnitude between healthy adults [54,55], and these values were therefore taken as variation between participants rather than as measurement error.

None of the three cortisol measures reached significance (Figure 7c,d). Daytime cortisol increased from a median of 1.941 to 2.266 ng/mg protein, but the change was not significant ($d = 0.37$; raw $p = 0.105$, $p_{adj} = 0.158$), and nighttime cortisol was essentially unchanged, from a median of 1.078 to 1.191 ng/mg protein ($d = -0.06$; raw $p = 0.524$, $p_{adj} = 0.628$). The daytime-dominant day–night difference (day minus night) increased from a median of 0.793 to 0.986 ng/mg protein, but the change was not significant ($d = 0.38$; raw $p = 0.092$, $p_{adj} = 0.158$). In the individual participant data, several participants showed large changes from baseline, but the direction of change differed across participants. In the primary analysis, among the six biomarker comparisons, the melatonin day–night difference

was the only change that reached significance after correction. When the same six comparisons were computed on the unnormalized concentrations, the melatonin day–night difference was again the only change significant after correction (p_{adj} = 0.028; Supplementary Table S4).

3.5. Safety Outcomes

No adverse skin reactions were reported during the 4-week application period.

3.6. Marker Content of the Liquid Preparation

Chlorogenic acid and rosmarinic acid, the marker compounds of the liquid preparation incorporated into the test cream, were quantified at 36 µg/g and 16 µg/g. Each peak was assigned by matching its retention time to that of the corresponding standard, run under identical conditions (Figure 8). These two compounds do not represent all six extracts. Chlorogenic acid has been reported as a constituent of loquat leaf [56], and rosmarinic acid as one of the principal constituents of rosemary [39]. The principal constituents named for the hop, chamomile, ginseng, and citrus peel components remain to be measured.

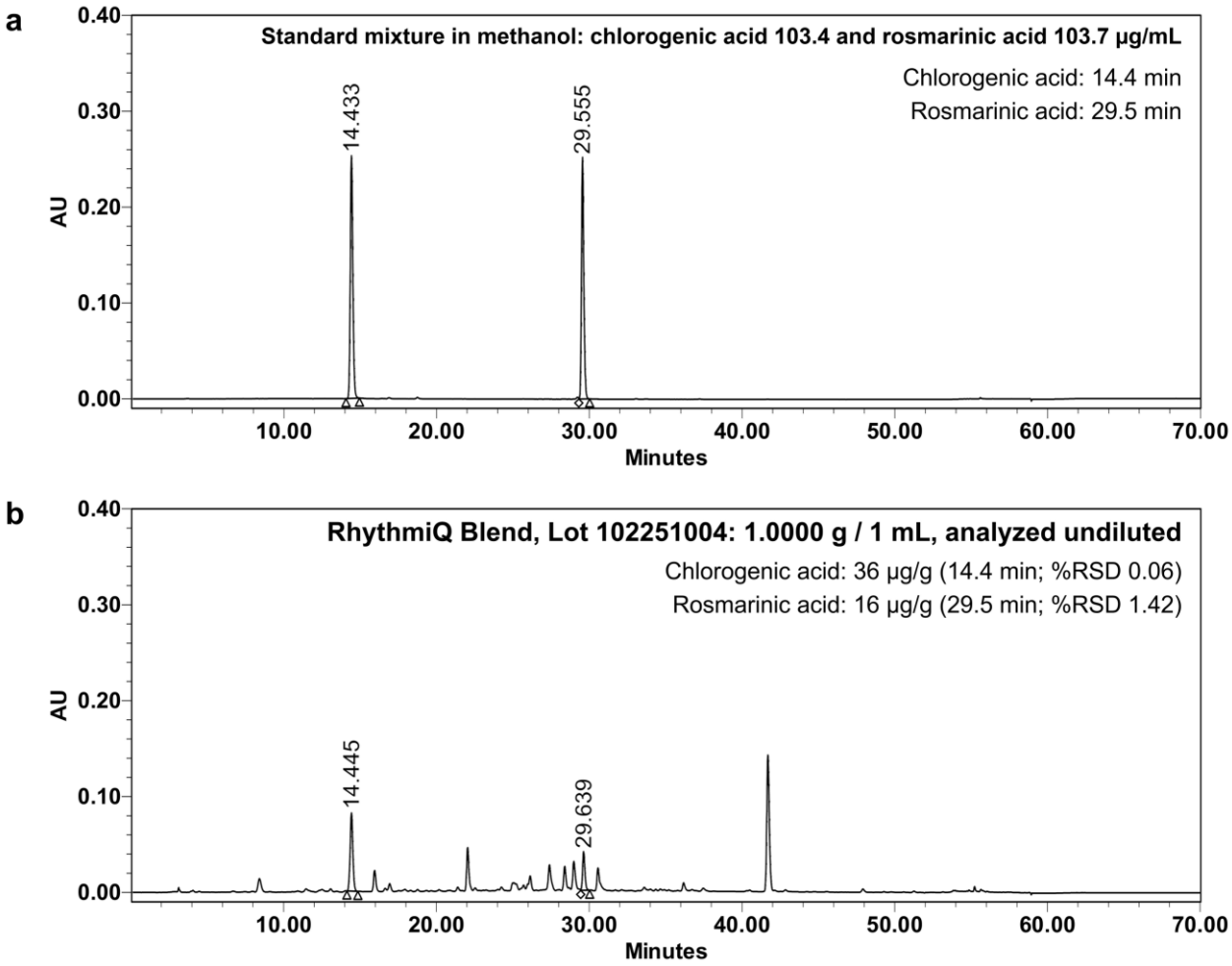


Figure 8. Chromatographic marker profile of the liquid preparation (Lot 102251004) incorporated into the test cream. (**a**) Standard mixture containing chlorogenic acid at 103.4 µg/mL and rosmarinic acid at 103.7 µg/mL in methanol. (**b**) The liquid preparation, analyzed undiluted. Chromatograms were recorded with photodiode-array detection at 325 nm; chlorogenic acid elutes at 14.4 min and rosmarinic acid at 29.5 min, and both were identified in the liquid preparation by comparison of retention time with the standards analyzed under the same conditions and quantified against five-

point external calibration curves (R [2] = 1.000). The contents determined were 36 μg/g for chlorogenic acid and 16 μg/g for rosmarinic acid, each the mean of three injections, with relative standard deviations of 0.06% and 1.42%, respectively. Peaks other than these two were not assigned.

4. Discussion

To date, what has less often been assembled is a single study that carries a molecular readout, the clinical skin outcomes, and objectively recorded extra-cutaneous measures on the same ingredient; a recent review of the skin–brain axis has identified this combination of dermatological, psychological, and biological outcome measures as a research need [33]. The present trial reports all three, with the clinical and extra-cutaneous measures taken in the same participants over the same 4 weeks; the limits of an uncontrolled pilot are considered below.

4.1. Principal Findings

In this cohort, change was most consistent in the skin: the 13 skin indicators changed significantly from baseline by week 4, and for 12 of the 13 the change was in the defined direction in all or all but one of the 22 participants, a consistency not matched in the wellness or salivary measures. The more informative feature, however, is not that each indicator changed but that change appeared at once in all four functional categories—anti-aging, barrier, complexion, and dark circles—which are ordinarily governed by different processes. One hypothesis compatible with this cross-category pattern is involvement of an upstream process such as the cutaneous clock.

The change was also ordered in time: 12 of the 13 indicators were already significant at week 2, and every indicator showed a numerically larger effect size at week 4 than at week 2, so the direction of change was set early and continued rather than emerging only at the final visit. The exception was the visual dark-circle grade, which reached significance only at week 4—the ordering expected of an integrative visual assessment relative to the instrumental measures that feed it, and the one indicator for which fewer than half the participants changed in the defined direction.

Changes were also recorded outside the skin over the same 4 weeks, in sleep duration, in the two questionnaire scores, and in the melatonin day–night difference. In these measures, however, the proportion of participants whose value changed in the defined direction was lower than for the instrumental skin indicators, and of the six salivary comparisons only the melatonin day–night difference reached significance after correction.

4.2. Clock-Associated Mechanism and Skin Outcomes

That the cutaneous clock could act upstream of outcomes in all four categories follows from the range of what it governs. The circadian machinery of the skin is not dedicated to a single function: it coordinates maintenance of the permeability barrier together with keratinocyte differentiation, dermal collagen remodeling governed by matrix metalloproteinase activity, antioxidant capacity coordinated through NRF2, and the setting of inflammatory tone by NF-κB signaling, the processes that sustain skin homeostasis over the 24 h cycle [9,14,17–19]. What the reporter assay reads is PER2 promoter-driven luciferase output, and constructs of this kind are used widely as a readout of core clock activity, PER2 being one component of the loop formed by BMAL1/CLOCK and the PER/CRY repressors [57]. Reading the reporter at that level, however, would require a change in the oscillation itself, since an effect on clock function is read from parameters of the oscillation, such as its amplitude, extracted from the detrended trace [58]. In our data, the amplitude and the overall output rose together; the result is an increase in *PER2* promoter-driven luciferase output rather than a demonstrated change in the rhythm. That output, in turn, is not separated from a direct effect on the firefly luciferase enzyme: compounds of the

kind present in plant extracts bind the enzyme directly [59], and such binding can raise the luminescent signal with no change in gene expression [60]. No luciferase control was performed in the present experiments, and the increase in reporter output therefore cannot be attributed solely to *PER2* promoter regulation. Settling whether a direct effect on the enzyme contributed would require a cell-free assay with purified firefly luciferase together with a construct driven by a constitutive promoter. Separately, endogenous *PER2* mRNA increased with the concentration of the mixture extract (Figure 2e), providing a luciferase-independent indication of increased *PER2* expression. However, this finding does not exclude a direct effect of the extract on the luciferase reporter signal. In addition, because endogenous *PER2* mRNA was measured only at discrete time points rather than continuously across a circadian cycle, these data do not establish an effect on *PER2* rhythmicity.

At the level of the cell, the keratinocyte observations suggest a more specific form for that upstream process. Treatment with the mixture extract raised *PER2* promoter-driven luciferase output and lowered *IL6* and *CXCL10*, and knockdown of *PER2* raised the same two transcripts. These observations are consistent with an association between *PER2* and inflammatory transcript expression in keratinocytes. Whether the suppression of *IL6* and *CXCL10* by the mixture extract is mediated by PER2 nonetheless remains a hypothesis rather than an established mechanism, because the two conditions were not examined in combination, and a contribution from PER2-independent signaling is still open. What would test it is to treat *PER2*-silenced cells with the mixture extract and to determine whether the suppression is maintained.

The place of the *IL6* and *CXCL10* measurements is nonetheless a limited one: they are a local keratinocyte inflammatory readout, one of the coordinated processes rather than the whole of it, and they were obtained in cell culture rather than in the participants. The two settings also differ in scale: the cell experiments used the mixture extract at 10 to 50 μg/mL, whereas the test cream contained it at 0.01% (*w*/*w*), that is 100 μg/g. Clock gene activity and inflammatory output were not measured in the skin of the participants, so the clock pathway stands as a candidate upstream process inferred from the clinical pattern rather than as a demonstrated cause of the change recorded across the 13 indicators. Recording clock gene activity and inflammatory output in treated skin would turn that account from an inference into a measurement.

4.3. Extra-Cutaneous Outcomes

Changes in the measures recorded outside the skin have been reported for topical products before: for a melatonin lotion, whose use was accompanied by changes in salivary melatonin and in sleep quality [61], for a fraction of tea tree essential oil, for which sleep quality and signs of skin aging were each assessed in a separate cohort [35], and for a tomato peel and seed extract, whose use was accompanied by lower salivary cortisol and improved affect [62]. In the present study, three measures outside the skin moved together with the skin indicators over the same 4 weeks: sleep duration increased, the PSQI-K score decreased and, among the salivary measures, the melatonin day–night difference increased, each significantly. A wearable record of time asleep, a questionnaire score, and a salivary difference are measurements of different kinds, so their concurrent movement does not rest on a single instrument or mode of reporting. Sleep and melatonin have been reported as parts of one physiological axis that extends to the circadian system regulating them [63], so a shift in that axis is one hypothesis compatible with this pattern. None of the three cortisol measures—the daytime concentration, the nighttime concentration, and the day–night difference between them—reached significance, so that change appeared in some of the salivary measures rather than across all of them. These observations do not identify a mechanism, but they point to melatonin-associated nighttime

physiology as the signal most worth testing. A study designed for that question would need salivary collection across the 24 h cycle, as would describing these hormones as circadian profiles; the single daytime and nighttime samples taken here support a day–night difference but not the shape of the nighttime rise.

4.4. Limitations and Future Directions

The design bounds what the changes can be attributed to. The study was single-arm and open-label and no blinding was applied: the participants knew that they were using an active product, and the staff who performed the measurements and their analysis, as well as the two evaluators who graded the dark-circle images, were aware of the visit number. On the measurement side, the sites were relocated at each visit, and the indicators whose relative change was smallest are the most exposed to the error that this introduces. Several sources of change therefore cannot be separated from an effect of the mixture extract. Placebo and expectancy effects bear on all of the outcomes and most directly on the two questionnaire scores. The vehicle is itself cosmetically active, since the base provides glycerin as a humectant and an emulsifier system that contributes shea butter, squalane and ceramide NP, so the barrier and complexion indicators may respond to the base as well as to the extract. Regression to the mean is particularly relevant to the PSQI-K score, because eligibility required an elevated baseline score. The trial ran from late October to late November, when daylength and sun exposure decrease, a seasonal course that could itself move skin color and melanin as well as melatonin and sleep. Participation may also have altered behavior—bedtime, evening light exposure, or facial care—in ways that were not recorded.

Given the pilot-sized cohort, dividing the available sample into parallel treatment and vehicle groups would have left very small groups for biomarkers with substantial between-participant variability. The amount of melatonin secreted differs by more than an order of magnitude across healthy adults, and daytime melatonin profiles are substantially heterogeneous [54,55]; for salivary cortisol, 10% to 15% of community samples have been found not to show the expected diurnal cycle at all [64]. We therefore used within-participant comparisons to reduce the contribution of between-participant differences and to characterize exploratory changes over time. This design improves precision for signal detection in a small pilot cohort but does not substitute for a randomized vehicle-controlled comparison. A split-face untreated control could have provided a local comparator for the skin outcomes, but it would not have provided an untreated comparator for the systemic sleep and salivary outcomes and was not included in this pilot study. The spread in the present cohort was of that order: at baseline the coefficient of variation was 225% and 99% for daytime and nighttime melatonin, against 57% and 70% for the corresponding cortisol measures. The expected day–night pattern was likewise not uniform: at baseline 10 of 22 participants had a nighttime melatonin concentration below their daytime concentration, whereas 4 of 22 showed the corresponding pattern for cortisol. The higher proportion of atypical melatonin day–night ordering may reflect heterogeneity in melatonin secretion or timing in this cohort; with only two sampling points, its origin cannot be determined. A small number of participants had markedly high baseline values; in a sensitivity analysis that reduced these values to the Tukey fence, the direction of the change, the number of participants whose value changed in the defined direction and the exclusion of zero from the unadjusted 95% confidence interval for the Hodges–Lehmann estimate were unchanged, whereas the magnitude of the estimate was smaller and, with the 1.5 × IQR fence, the adjusted p-value no longer met the significance criterion. We retained all observations and treated this spread as variation between participants rather than as measurement error. Values that depart from the group pattern may themselves be informative for further study of salivary melatonin in people with poor sleep quality.

What the present design could not resolve is between-participant structure: a cohort recruited on a self-reported behavioral criterion may be uniform in what its members report while remaining heterogeneous in the underlying physiology that a clock-oriented ingredient is directed at. Whether the changes depended on the baseline level is worth examining, although a single-arm design cannot separate a genuinely baseline-dependent pattern from the regression already noted. Stratification by baseline phenotype is therefore worth building into the design of the trial that should follow, and there is precedent for expecting it to matter: response to prolonged-release melatonin has been reported to depend on endogenous concentrations [65], and patient-level meta-analysis has shown treatment response to be conditioned by baseline severity [66]. That trial should be randomized, vehicle-controlled and blinded, on the larger sample that a between-group comparison of the salivary measures requires.

A further set of limits concerns not the cause of the changes but their reach. The observation period was 4 weeks, and the cohort comprised women aged 40 to 70 years with a PSQI-K score of 7 or higher, the population in which the question was posed. The 4-week period and this cohort mark the range over which these changes have been observed, not a range beyond which they are known to fail; establishing that range would require longer follow-up and broader recruitment.

5. Conclusions

The present study found that, in HaCaT keratinocytes, a six-botanical mixture extract raised *PER2* promoter-driven luciferase output and lowered *IL6* and *CXCL10* expression. The clinical part, conducted separately, was a 4-week, single-arm, open-label pilot in which a clock-oriented topical cosmetic—a cream containing a liquid preparation of that extract—was applied nightly to the face by 22 women aged 40 to 70 years with poor sleep quality. Change from baseline was recorded across the instrumental skin indicators and, outside the skin, in sleep duration, the sleep-quality and mood questionnaire scores, and the melatonin day–night difference, but not in the cortisol measures.

What this design supports is a statement about concurrence rather than causation: with no control group, the alternative sources of change set out above remain open, and these are exploratory findings. Neither the efficacy of the formulation nor a PER2-mediated mechanism is settled here; what the study does show is that the skin indicators and the measures recorded outside the skin changed over the same 4-week period. The value of the present work for the randomized, vehicle-controlled trial that should follow is that it fixes the outcome set to be measured and identifies melatonin-associated nighttime physiology as the extra-cutaneous signal most worth testing.

Supplementary Materials: The following supporting information can be downloaded at https://www.mdpi.com/article/10.3390/cosmetics13060301/s1, Table S1: In vitro assays of the six-botanical mixture extract in HaCaT keratinocytes; Table S2: Skin outcome indicators before and after treatment (N = 22); Table S3: Wellness indicators before and after treatment (N = 22); Table S4: Salivary biomarkers before and after treatment (N = 22), normalized to total protein and as unnormalized concentrations; Table S5: Sensitivity of the melatonin day–night difference to high baseline concentrations (N = 22); File S1: TREND Statement Checklist. Reference [67] is cited in the Supplementary Materials.

Author Contributions: Conceptualization, M.Y. and E.J.; methodology, M.Y. and S.M.; investigation, M.Y., S.M., Y.J.J. and S.C.; resources, Y.J. and E.C.; validation, K.J. and D.-H.R.; formal analysis, M.Y., H.K. and E.J.; data curation, M.Y., Y.J.J. and S.C.; writing—original draft preparation, M.Y.; writing—review and editing, E.J. and D.P.; visualization, M.Y.; supervision, E.J. and D.P.; project

administration, E.J.; funding acquisition, E.J. All authors have read and agreed to the published version of the manuscript.

Funding: This research was funded by the Technology Development Program of the Ministry of SMEs and Startups (MSS), Republic of Korea, grant number S3430878.

Institutional Review Board Statement: The study was conducted in accordance with the Declaration of Helsinki and approved by the Institutional Review Board of Dermacle Co., Ltd. (protocol code DM-IRB-2025-1014-04, approved on 17 October 2025). The trial was registered at the Clinical Research Information Service of the Republic of Korea (KCT0011193). Cell information: HaCaT (CLS Cell Line Service GmbH, Eppelheim, Germany); HaCaT-derived reporter line stably expressing a *PER2* promoter–driven luciferase construct (PER2pro-LUC).

Informed Consent Statement: Informed consent was obtained from all subjects involved in the study. Written informed consent has been obtained from the participants whose images are shown in Figure 5c to publish this paper.

Data Availability Statement: The data presented in this study are available upon request from the corresponding author. The data are not publicly available due to commercial confidentiality.

Acknowledgments: The authors thank all participants in this study. The graphical abstract was created in BioRender. Jung, E. (2026) (https://BioRender.com/cfhq0p4). During the preparation of this manuscript, the authors used Claude Opus 5 (Anthropic) for the purposes of polishing the language of the manuscript. The authors have reviewed and edited the output and take full responsibility for the content of this publication.

Conflicts of Interest: Authors M.Y., Y.J., K.J., S.M., D.-H.R., E.C., D.P. and E.J. were employed by the company BioSpectrum Inc., which developed and manufacture the test materials. Authors Y.J.J., S.C. and H.K. were employed by Dermacle Skin Research Center for Clinical Test of Cosmetics, the institution that conducted the clinical evaluation. All authors therefore have a commercial affiliation, and these affiliations are declared here as potential conflicts of interest. The authors declare that this study received funding from the Ministry of SMEs and Startups, Republic of Korea. The funder was not involved in the study design, collection, analysis, interpretation of data, the writing of this article, or the decision to submit it for publication. The funder did not affect the experimental process and results in the study. The funding relationship does not affect the scientific quality of the manuscript.

Abbreviations

ANOVA	analysis of variance
BCA	bicinchoninic acid
BH	Benjamini–Hochberg
CRIS	Clinical Research Information Service
CXCL-10	C-X-C motif chemokine ligand 10
DMEM	Dulbecco's Modified Eagle's Medium
DMSO	dimethyl sulfoxide
ELISA	enzyme-linked immunosorbent assay
FBS	fetal bovine serum
FFT NLLS	fast Fourier transform–nonlinear least squares
IL-6	interleukin-6
INCI	International Nomenclature of Cosmetic Ingredients
MMP-1	matrix metalloproteinase-1
MTT	3-(4,5-dimethylthiazol-2-yl)-2,5-diphenyltetrazolium bromide
PER2pro-LUC	*PER2* promoter–driven luciferase construct
PHQ-9	Patient Health Questionnaire-9
PSQI-K	Korean version of the Pittsburgh Sleep Quality Index

RT-PCR	reverse transcription polymerase chain reaction
SCN	suprachiasmatic nucleus
SD	standard deviation
SEM	standard error of the mean
siRNA	small interfering RNA
TEWL	transepidermal water loss

References

1. Knaggs, H.; Lephart, E.D. Enhancing Skin Anti-Aging through Healthy Lifestyle Factors. *Cosmetics* **2023**, *10*, 142. https://doi.org/10.3390/cosmetics10050142.
2. Oyetakin-White, P.; Suggs, A.; Koo, B.; Matsui, M.S.; Yarosh, D.; Cooper, K.D.; Baron, E.D. Does Poor Sleep Quality Affect Skin Ageing? *Clin. Exp. Dermatol.* **2015**, *40*, 17–22. https://doi.org/10.1111/ced.12455.
3. Jang, S.I.; Jung, Y.; Lee, M.; Kim, J.; Kim, B.J.; Suh, B.; Kim, E. Evaluation of Changes in Skin Characteristics Due to the Poor Quality of Sleep Caused by Smartphone Usage. *J. Cosmet. Dermatol.* **2022**, *21*, 1656–1665. https://doi.org/10.1111/jocd.14265.
4. Axelsson, J.; Sundelin, T.; Ingre, M.; Van Someren, E.J.W.; Olsson, A.; Lekander, M. Beauty Sleep: Experimental Study on the Perceived Health and Attractiveness of Sleep Deprived People. *BMJ* **2010**, *341*, c6614. https://doi.org/10.1136/bmj.c6614.
5. Sundelin, T.; Lekander, M.; Kecklund, G.; Van Someren, E.J.W.; Olsson, A.; Axelsson, J. Cues of Fatigue: Effects of Sleep Deprivation on Facial Appearance. *Sleep* **2013**, *36*, 1355–1360. https://doi.org/10.5665/sleep.2964.
6. Altemus, M.; Rao, B.; Dhabhar, F.S.; Ding, W.; Granstein, R.D. Stress-Induced Changes in Skin Barrier Function in Healthy Women. *J. Investig. Dermatol.* **2001**, *117*, 309–317. https://doi.org/10.1046/j.1523-1747.2001.01373.x.
7. Jang, S.I.; Lee, M.; Han, J.; Kim, J.; Kim, A.R.; An, J.S.; Park, J.O.; Kim, B.J.; Kim, E. A Study of Skin Characteristics with Long-Term Sleep Restriction in Korean Women in Their 40s. *Skin Res. Technol.* **2020**, *26*, 193–199. https://doi.org/10.1111/srt.12797.
8. Irwin, M.R.; Olmstead, R.; Carroll, J.E. Sleep Disturbance, Sleep Duration, and Inflammation: A Systematic Review and Meta-Analysis of Cohort Studies and Experimental Sleep Deprivation. *Biol. Psychiatry* **2016**, *80*, 40–52. https://doi.org/10.1016/j.biopsych.2015.05.014.
9. Duan, J.; Greenberg, E.N.; Karri, S.S.; Andersen, B. The Circadian Clock and Diseases of the Skin. *FEBS Lett.* **2021**, *595*, 2413–2436. https://doi.org/10.1002/1873-3468.14192.
10. Möller-Levet, C.S.; Archer, S.N.; Bucca, G.; Laing, E.E.; Slak, A.; Kabiljo, R.; Lo, J.C.Y.; Santhi, N.; von Schantz, M.; Smith, C.P.; et al. Effects of Insufficient Sleep on Circadian Rhythmicity and Expression Amplitude of the Human Blood Transcriptome. *Proc. Natl. Acad. Sci. USA* **2013**, *110*, E1132–E1141. https://doi.org/10.1073/pnas.1217154110.
11. Archer, S.N.; Laing, E.E.; Möller-Levet, C.S.; van der Veen, D.R.; Bucca, G.; Lazar, A.S.; Santhi, N.; Slak, A.; Kabiljo, R.; von Schantz, M.; et al. Mistimed Sleep Disrupts Circadian Regulation of the Human Transcriptome. *Proc. Natl. Acad. Sci. USA* **2014**, *111*, E682–E691. https://doi.org/10.1073/pnas.1316335111.
12. Shao, Q.; Wang, Z.; Li, Y.; Tang, X.; Li, Z.; Xia, H.; Wu, Q.; Chang, R.; Wu, C.; Meng, T.; et al. Taurine Prevents Impairments in Skin Barrier Function and Dermal Collagen Synthesis Triggered by Sleep Deprivation-Induced Estrogen Circadian Rhythm Disruption. *Cells* **2025**, *14*, 727. https://doi.org/10.3390/cells14100727.
13. Li, W.; Wang, Z.; Cao, J.; Dong, Y.; Chen, Y. Melatonin Improves Skin Barrier Damage Caused by Sleep Restriction through Gut Microbiota. *J. Pineal Res.* **2023**, *75*, e12874. https://doi.org/10.1111/jpi.12874.
14. Sherratt, M.J.; Hopkinson, L.; Naven, M.; Hibbert, S.A.; Ozols, M.; Eckersley, A.; Newton, V.L.; Bell, M.; Meng, Q.-J. Circadian Rhythms in Skin and Other Elastic Tissues. *Matrix Biol.* **2019**, *84*, 97–110. https://doi.org/10.1016/j.matbio.2019.08.004.
15. Hettwer, S.; Besic Gyenge, E.; Obermayer, B. Influence of Cosmetic Formulations on the Skin's Circadian Clock. *Int. J. Cosmet. Sci.* **2020**, *42*, 313–319. https://doi.org/10.1111/ics.12623.
16. del Olmo, M.; Spörl, F.; Korge, S.; Jürchott, K.; Felten, M.; Grudziecki, A.; de Zeeuw, J.; Nowozin, C.; Reuter, H.; Blatt, T.; et al. Inter-Layer and Inter-Subject Variability of Diurnal Gene Expression in Human Skin. *NAR Genom. Bioinform.* **2022**, *4*, lqac097. https://doi.org/10.1093/nargab/lqac097.
17. Frigato, E.; Benedusi, M.; Guiotto, A.; Bertolucci, C.; Valacchi, G. Circadian Clock and OxInflammation: Functional Crosstalk in Cutaneous Homeostasis. *Oxid. Med. Cell. Longev.* **2020**, *2020*, 2309437. https://doi.org/10.1155/2020/2309437.
18. Paatela, E.; Munson, D.; Kikyo, N. Circadian Regulation in Tissue Regeneration. *Int. J. Mol. Sci.* **2019**, *20*, 2263. https://doi.org/10.3390/ijms20092263.
19. Németh, V.; Horváth, S.; Kinyó, Á.; Gyulai, R.; Lengyel, Z. Expression Patterns of Clock Gene mRNAs and Clock Proteins in Human Psoriatic Skin Samples. *Int. J. Mol. Sci.* **2022**, *23*, 121. https://doi.org/10.3390/ijms23010121.

20. Yeom, M.; Lee, H.; Shin, S.; Park, D.; Jung, E. PER, a Circadian Clock Component, Mediates the Suppression of MMP-1 Expression in HaCaT Keratinocytes by cAMP. *Molecules* **2018**, *23*, 745. https://doi.org/10.3390/molecules23040745.
21. Kim, J.-Y.; Lee, J.; Lee, S.-H.; Jung, E.-M.; Lee, K.-H. Modulatory Effects of Cinnamomi Cortex and Its Components Epicatechin and Linalool on Skin Circadian Rhythms. *Sci. Rep.* **2025**, *15*, 4480. https://doi.org/10.1038/s41598-025-88325-5.
22. Yeom, M.; Jeon, K.; Ryu, D.-H.; Park, D.; Jung, E. Time-of-Day Dependent Promotion of Keratinocyte Differentiation by *Cinnamomum cassia* Bark Extract through the P38 MAPK Pathway. *PLoS ONE* **2025**, *20*, e0318360. https://doi.org/10.1371/journal.pone.0318360.
23. Hardman, J.A.; Tobin, D.J.; Haslam, I.S.; Farjo, N.; Farjo, B.; Al-Nuaimi, Y.; Grimaldi, B.; Paus, R. The Peripheral Clock Regulates Human Pigmentation. *J. Investig. Dermatol.* **2015**, *135*, 1053–1064. https://doi.org/10.1038/jid.2014.442.
24. Geyfman, M.; Kumar, V.; Liu, Q.; Ruiz, R.; Gordon, W.; Espitia, F.; Cam, E.; Millar, S.E.; Smyth, P.; Ihler, A.; et al. Brain and Muscle Arnt-like Protein-1 (BMAL1) Controls Circadian Cell Proliferation and Susceptibility to UVB-Induced DNA Damage in the Epidermis. *Proc. Natl. Acad. Sci. USA* **2012**, *109*, 11758–11763. https://doi.org/10.1073/pnas.1209592109.
25. Silveira, E.J.D.; Nascimento Filho, C.H.V.; Yujra, V.Q.; Webber, L.P.; Castilho, R.M.; Squarize, C.H. BMAL1 Modulates Epidermal Healing in a Process Involving the Antioxidative Defense Mechanism. *Int. J. Mol. Sci.* **2020**, *21*, 901. https://doi.org/10.3390/ijms21030901.
26. Yosipovitch, G.; Xiong, G.L.; Haus, E.; Sackett-Lundeen, L.; Ashkenazi, I.; Maibach, H.I. Time-Dependent Variations of the Skin Barrier Function in Humans: Transepidermal Water Loss, Stratum Corneum Hydration, Skin Surface pH, and Skin Temperature. *J. Investig. Dermatol.* **1998**, *110*, 20–23. https://doi.org/10.1046/j.1523-1747.1998.00069.x.
27. Slominski, R.M.; Raman, C.; Jetten, A.M.; Slominski, A.T. Neuro–Immuno–Endocrinology of the Skin: How Environment Regulates Body Homeostasis. *Nat. Rev. Endocrinol.* **2025**, *21*, 495–509. https://doi.org/10.1038/s41574-025-01107-x.
28. Ascsillán, A.A.; Kemény, L.V. The Skin–Brain Axis: From UV and Pigmentation to Behaviour Modulation. *Int. J. Mol. Sci.* **2024**, *25*, 6199. https://doi.org/10.3390/ijms25116199.
29. Chen, Y.-Y.; Liu, L.-P.; Zhou, H.; Zheng, Y.-W.; Li, Y.-M. Recognition of Melanocytes in Immuno-Neuroendocrinology and Circadian Rhythms: Beyond the Conventional Melanin Synthesis. *Cells* **2022**, *11*, 2082. https://doi.org/10.3390/cells11132082.
30. Zhang, H.; Wang, M.; Zhao, X.; Wang, Y.; Chen, X.; Su, J. Role of Stress in Skin Diseases: A Neuroendocrine-Immune Interaction View. *Brain Behav. Immun.* **2024**, *116*, 286–302. https://doi.org/10.1016/j.bbi.2023.12.005.
31. Misery, L.; Pierre, O.; Le Gall-Ianotto, C.; Lebonvallet, N.; Chernyshov, P.V.; Le Garrec, R.; Talagas, M. Basic Mechanisms of Itch. *J. Allergy Clin. Immunol.* **2023**, *152*, 11–23. https://doi.org/10.1016/j.jaci.2023.05.004.
32. Stenger, S.; Grasshoff, H.; Hundt, J.E.; Lange, T. Potential Effects of Shift Work on Skin Autoimmune Diseases. *Front. Immunol.* **2023**, *13*, 1000951. https://doi.org/10.3389/fimmu.2022.1000951.
33. Marano, G.; Giacomi, O.D.; Lanzetta, M.; Scialpi, C.; Sottile, A.; Traversi, G.; Mazza, O.; d'Abate, C.; Gaetani, E.; Mazza, M. Neurocosmetics and the Skin-Brain Axis from a Psychological and Psychiatric Standpoint. *Cosmetics* **2026**, *13*, 102. https://doi.org/10.3390/cosmetics13030102.
34. Merola, J.F.; Chiou, A.S.; During, E.; Costanzo, A.; Foley, P.; Alfalasi, A.; Gogate, S.; Pinter, A.; Dodiuk-Gad, R.; Simon, D.; et al. Dupilumab Significantly Improves Sleep in Adults with Atopic Dermatitis: Results from the 12-Week Placebo-Controlled Period of the 24-Week Phase IV Randomized Double-Blinded Placebo-Controlled DUPISTAD Study. *Br. J. Dermatol.* **2023**, *189*, 685–694. https://doi.org/10.1093/bjd/ljad284.
35. Duroux, R.; Jain, A.; Tabert, M.; Attia, J. An Upcycled Fraction of Melaleuca Alternifolia Essential Oil Regenerates the Skin through the Skin Melatonin Pathway and Improves Sleep Quality. *J. Cosmet. Dermatol.* **2024**, *23*, 1840–1849. https://doi.org/10.1111/jocd.16179.
36. Weber, N.; Biehler, K.; Schwabe, K.; Haarhaus, B.; Quirin, K.-W.; Frank, U.; Schempp, C.M.; Wölfle, U. Hop Extract Acts as an Antioxidant with Antimicrobial Effects against *Propionibacterium acnes* and *Staphylococcus aureus*. *Molecules* **2019**, *24*, 223. https://doi.org/10.3390/molecules24020223.
37. Chen, G.; Lv, C.; Nie, Q.; Li, X.; Lv, Y.; Liao, G.; Liu, S.; Ge, W.; Chen, J.; Du, Y. Essential Oil of *Matricaria chamomilla* Alleviate Psoriatic-like Skin Inflammation by Inhibiting PI3K/Akt/mTOR and p38MAPK Signaling Pathway. *Clin. Cosmet. Investig. Dermatol.* **2024**, *17*, 59–77. https://doi.org/10.2147/CCID.S445008.
38. Park, J.J.; An, J.; Lee, J.D.; Kim, H.Y.; Im, J.E.; Lee, E.; Ha, J.; Cho, C.H.; Seo, D.-W.; Kim, K.-B. Effects of Anti-Wrinkle and Skin-Whitening Fermented Black Ginseng on Human Subjects and Underlying Mechanism of Action. *J. Toxicol. Environ. Health A* **2020**, *83*, 423–437. https://doi.org/10.1080/15287394.2020.1776454.

39. Kasamatsu, S.; Takano, K.; Aoki, M.; Takahashi, Y.; Suzuki, T. Rosemary Extract and Rosmarinic Acid Accelerate Elastic Fiber Formation by Increasing the Expression of Elastic Fiber Components in Dermal Fibroblasts. *J. Dermatol.* **2024**, *51*, 816–826. https://doi.org/10.1111/1346-8138.17185.
40. Tan, H.; Sonam, T.; Shimizu, K. The Potential of Triterpenoids from Loquat Leaves (*Eriobotrya japonica*) for Prevention and Treatment of Skin Disorder. *Int. J. Mol. Sci.* **2017**, *18*, 1030. https://doi.org/10.3390/ijms18051030.
41. Bae, J.T.; Ko, H.J.; Kim, G.B.; Pyo, H.B.; Lee, G.S. Protective Effects of Fermented *Citrus unshiu* Peel Extract against Ultraviolet-A-Induced Photoageing in Human Dermal Fibroblasts. *Phytother. Res.* **2012**, *26*, 1851–1856. https://doi.org/10.1002/ptr.4670.
42. Buysse, D.J.; Reynolds, C.F.; Monk, T.H.; Berman, S.R.; Kupfer, D.J. The Pittsburgh Sleep Quality Index: A New Instrument for Psychiatric Practice and Research. *Psychiatry Res.* **1989**, *28*, 193–213. https://doi.org/10.1016/0165-1781(89)90047-4.
43. Sohn, S.I.; Kim, D.H.; Lee, M.Y.; Cho, Y.W. The Reliability and Validity of the Korean Version of the Pittsburgh Sleep Quality Index. *Sleep Breath.* **2012**, *16*, 803–812. https://doi.org/10.1007/s11325-011-0579-9.
44. Lee, S.Y.; Choi, J.E.; Lee, J.W.; Lee, Y.; Park, J.M.; Hong, K.W. Testing the Reliability and Validity of the Korean Version of the Pittsburgh Sleep Quality Index Using Fitbit Devices: A Cross-Sectional Analysis. *Korean J. Fam. Med.* **2025**, *46*, 42–47. https://doi.org/10.4082/kjfm.23.0166.
45. Kim, J.K.; Lim, S.H.; Kim, W.G.; Cho, C.; Ha, J.; Seo, D.B. Beneficial Effect of Collagen-Peptide Mixture with GABA on Improvement Skin and Sleep Quality. *J. Soc. Cosmet. Sci. Korea* **2018**, *44*, 277–284. https://doi.org/10.15230/SCSK.2018.44.3.277.
46. Rodrigues, L.; EEMCO Group. EEMCO Guidance to the in Vivo Assessment of Tensile Functional Properties of the Skin. Part 2: Instrumentation and Test Modes. *Skin Pharmacol. Appl. Skin Physiol.* **2001**, *14*, 52–67. https://doi.org/10.1159/000056334.
47. Lee, P.H. Number of Days Required to Reliably Measure Weekday and Weekend Total Sleeping Time with Accelerometer: A Secondary Data Analysis with National Health and Nutritional Survey (NHANES) 2011–2014 Data. *Sleep Med.* **2024**, *114*, 178–181. https://doi.org/10.1016/j.sleep.2024.01.006.
48. Kroenke, K.; Spitzer, R.L.; Williams, J.B.W. The PHQ-9: Validity of a Brief Depression Severity Measure. *J. Gen. Intern. Med.* **2001**, *16*, 606–613. https://doi.org/10.1046/j.1525-1497.2001.016009606.x.
49. Jeamanukulkit, S.; Vichayanrat, T.; Samnieng, P. Effects of the Salivary Gland Massage Program in Older Type 2 Diabetes Patients on the Salivary Flow Rate, Xerostomia, Swallowing and Oral Hygiene: A Randomized Controlled Trial. *Geriatr. Gerontol. Int.* **2023**, *23*, 549–557. https://doi.org/10.1111/ggi.14629.
50. Zhu, C.; Yuan, C.; Ren, Q.; Wei, F.; Yu, S.; Sun, X.; Zheng, S. Comparative Analysis of the Effects of Collection Methods on Salivary Steroids. *BMC Oral Health* **2021**, *21*, 352. https://doi.org/10.1186/s12903-021-01722-w.
51. Moraes, M.M.; Marques, A.L.; Borges, L.; Hatanaka, E.; Heller, D.; Núñez-Espinosa, C.; Gonçalves, D.A.P.; Soares, D.D.; Wanner, S.P.; Mendes, T.T.; et al. Sleep Impairment and Altered Pattern of Circadian Biomarkers during a Long-Term Antarctic Summer Camp. *Sci. Rep.* **2023**, *13*, 15959. https://doi.org/10.1038/s41598-023-42910-8.
52. Lakens, D. Calculating and Reporting Effect Sizes to Facilitate Cumulative Science: A Practical Primer for t-Tests and ANOVAs. *Front. Psychol.* **2013**, *4*, 863. https://doi.org/10.3389/fpsyg.2013.00863.
53. Cohen, J. *Statistical Power Analysis for the Behavioral Sciences*, 2nd ed.; Lawrence Erlbaum Associates: Hillsdale, NJ, USA, 1988; ISBN 0-8058-0283-5.
54. Burgess, H.J.; Fogg, L.F. Individual Differences in the Amount and Timing of Salivary Melatonin Secretion. *PLoS ONE* **2008**, *3*, e3055. https://doi.org/10.1371/journal.pone.0003055.
55. Bouwmans, M.E.J.; Bos, E.H.; Booij, S.H.; van Faassen, M.; Oldehinkel, A.J.; de Jonge, P. Intra- and Inter-Individual Variability of Longitudinal Daytime Melatonin Secretion Patterns in Depressed and Non-Depressed Individuals. *Chronobiol. Int.* **2014**, *32*, 441–446. https://doi.org/10.3109/07420528.2014.973114.
56. Jung, H.A.; Park, J.C.; Chung, H.Y.; Kim, J.; Choi, J.S. Antioxidant Flavonoids and Chlorogenic Acid from the Leaves of *Eriobotrya japonica*. *Arch. Pharm. Res.* **1999**, *22*, 213–218. https://doi.org/10.1007/BF02976549.
57. Yoo, S.-H.; Ko, C.H.; Lowrey, P.L.; Buhr, E.D.; Song, E.; Chang, S.; Yoo, O.J.; Yamazaki, S.; Lee, C.; Takahashi, J.S. A Noncanonical E-Box Enhancer Drives Mouse Period2 Circadian Oscillations In Vivo. *Proc. Natl. Acad. Sci. USA* **2005**, *102*, 2608–2613. https://doi.org/10.1073/pnas.0409763102.
58. Zhang, E.E.; Liu, A.C.; Hirota, T.; Miraglia, L.J.; Welch, G.; Pongsawakul, P.Y.; Liu, X.; Atwood, A.; Huss, J.W.; Janes, J.; et al. A Genome-Wide RNAi Screen for Modifiers of the Circadian Clock in Human Cells. *Cell* **2009**, *139*, 199–210. https://doi.org/10.1016/j.cell.2009.08.031.
59. Kenda, M.; Vegelj, J.; Herlah, B.; Perdih, A.; Mladěnka, P.; Sollner Dolenc, M. Evaluation of Firefly and Renilla Luciferase Inhibition in Reporter-Gene Assays: A Case of Isoflavonoids. *Int. J. Mol. Sci.* **2021**, *22*, 6927. https://doi.org/10.3390/ijms22136927.

60. Thorne, N.; Shen, M.; Lea, W.A.; Simeonov, A.; Lovell, S.; Auld, D.S.; Inglese, J. Firefly Luciferase in Chemical Biology: A Compendium of Inhibitors, Mechanistic Evaluation of Chemotypes, and Suggested Use as a Reporter. *Chem. Biol.* **2012**, *19*, 1060–1072. https://doi.org/10.1016/j.chembiol.2012.07.015.
61. Ponce, C.; Razon, A.D.; Chao, J.; Nakagawa, S.K.; Peterson, M.M.; Roque, A.Y.; Vanderpool, M.A.; Ferracane, M.J.; Olson, L.E. Impact of an Over-the-Counter "Sleep Lotion" on Human Salivary Melatonin Levels and Sleep Quality: A Randomized Controlled Trial. *Neuro Endocrinol. Lett.* **2024**, *45*, 167–172.
62. Falcao, L.; Nachat-Kappes, R.; Filaire, E. In and out Beauty and Sensitive Skin, a Psychophysiological Exploration: Myth or Reality? *Cosmetics* **2024**, *11*, 36. https://doi.org/10.3390/cosmetics11020036.
63. Zisapel, N. New Perspectives on the Role of Melatonin in Human Sleep, Circadian Rhythms and Their Regulation. *Br. J. Pharmacol.* **2018**, *175*, 3190–3199. https://doi.org/10.1111/bph.14116.
64. Stone, A.A.; Schwartz, J.E.; Smyth, J.; Kirschbaum, C.; Cohen, S.; Hellhammer, D.; Grossman, S. Individual Differences in the Diurnal Cycle of Salivary Free Cortisol: A Replication of Flattened Cycles for Some Individuals. *Psychoneuroendocrinology* **2001**, *26*, 295–306. https://doi.org/10.1016/s0306-4530(00)00057-3.
65. Wade, A.G.; Ford, I.; Crawford, G.; McConnachie, A.; Nir, T.; Laudon, M.; Zisapel, N. Nightly Treatment of Primary Insomnia with Prolonged Release Melatonin for 6 Months: A Randomized Placebo Controlled Trial on Age and Endogenous Melatonin as Predictors of Efficacy and Safety. *BMC Med.* **2010**, *8*, 51. https://doi.org/10.1186/1741-7015-8-51.
66. Fournier, J.C.; DeRubeis, R.J.; Hollon, S.D.; Dimidjian, S.; Amsterdam, J.D.; Shelton, R.C.; Fawcett, J. Antidepressant Drug Effects and Depression Severity: A Patient-Level Meta-Analysis. *JAMA* **2010**, *303*, 47–53. https://doi.org/10.1001/jama.2009.1943.
67. Des Jarlais, D.C.; Lyles, C.; Crepaz, N.; TREND Group. Improving the Reporting Quality of Nonrandomized Evaluations of Behavioral and Public Health Interventions: The TREND Statement. *Am. J. Public Health* **2004**, *94*, 361–366. https://doi.org/10.2105/AJPH.94.3.361.

Disclaimer/Publisher's Note: The statements, opinions and data contained in all publications are solely those of the individual author(s) and contributor(s) and not of MDPI and/or the editor(s). MDPI and/or the editor(s) disclaim responsibility for any injury to people or property resulting from any ideas, methods, instructions or products referred to in the content.